

**FULLY PRINTABLE CHIPLESS RFID TAG WITH INTEGRATED  
SENSORS**



by

**NS Muhammad Tanzeel Khalid**

00000320105/MSEE25

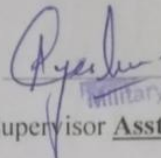
Supervisor

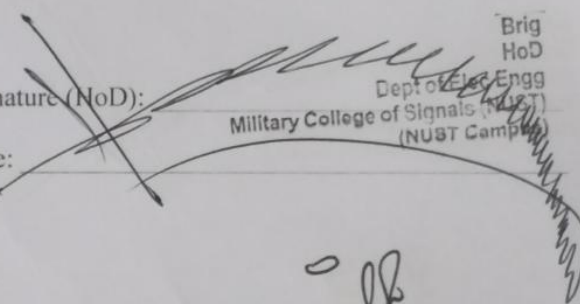
**Asst Prof Ayesha Habib, PhD**

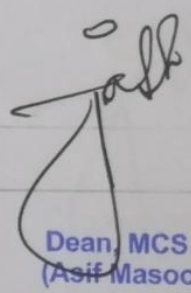
A thesis submitted in conformity with the requirements for the degree of Master of Science in Electrical (Telecom) Engineering, Department of Electrical (Telecom) Engineering, Military College of Signals (MCS), National University of Sciences and Technology (NUST), Islamabad, Pakistan.

**THESIS ACCEPTANCE CERTIFICATE**

Certified that final copy of MS/MPhil thesis written by Mr. **NS Muhammad Tanzeel Khalid**, Registration No. **00000320105** of **Military College of Signals** has been vetted by undersigned, found complete in all respect as per NUST Statutes/Regulations, is free of plagiarism, errors and mistakes and is accepted as partial, fulfillment for award of MS/MPhil degree. It is further certified that necessary amendments as pointed out by GEC members of the student have been also incorporated in the said thesis.

Signature:  **Assoc HoD  
Dept of Elec Engg  
Military College of Signals  
(NUST Campus)**  
Name of Supervisor **Asst Prof Ayesha Habib, PhD**  
Date: \_\_\_\_\_

Signature (HoD):  **Brig  
HoD  
Dept of Elec Engg  
Military College of Signals (NUST)  
(NUST Campus)**  
Date: \_\_\_\_\_

Signature (Dean):  \_\_\_\_\_  
Date: **18/7/23** \_\_\_\_\_  
**Brig  
Dean, MCS (NUST)  
(Asif Masood, PhD)**

## ABSTRACT

In this research work, 30-bit Chipless RFID tag with humidity sensing capability is presented. Tag basically comprised of two triangular patches named patch A and patch B arranged in a fan shaped manner, thus making it capable for long read range applications. To make the tag suitable for different environmental conditions, Various substrates including Taconic (TLX-8), PET, Rogers RT/Duroid® (5880) and Kapton® HN are used to examine the tag. The final tag is designed on Dupont Kapton® HN in which silver nanoparticle ink is used as radiator. A 55.3 x 55.3 mm<sup>2</sup> tag design with a operating frequency range of 2.63 to 9.22 GHz is intended. To ensure the printability and flexibility of the tag, silver nano particle is used as the radiator and Kapton® HN as the substrate. This Kapton® HN substrate based Chipless RFID tag also shows the humidity sensing property along with the better-read range capacity. For low-cost item tagging items, this tag can be the best choice.

## **DECLARATION**

I affirm that the work "Fully Printable Chipless RFID Tag with Integrated Sensors" presented in this thesis was not submitted in support of any other prize or academic credential, either at this school or elsewhere.

## **DEDICATION**

This thesis is dedicated to

**MY BELOVED PARENTS, HONORABLE TEACHERS**

**AND FRIENDS** for their love, endless support, and

encouragement

## ACKNOWLEDGEMENTS

All praise belongs to the Powerful Allah, WHO has given me the courage and resilience to accomplish my objectives. I want to start by sincerely thanking my co-supervisor, Dr. Mir Yasir Umair, and my devoted and revered supervisor, Dr. Ayesha Habib, for their support, collaboration, and guidance throughout the completion of my thesis. They generously offered to supervise me as I worked on my thesis and greatly assisted me in finishing my study. Additionally, I would like to express my gratitude to my committee members for their assistance and insightful comments on my study. Last but not least, I would like to thank my parents and siblings, **to** whom I am dedicating this effort, from the bottom of my heart. Without their generous assistance, prayers, and encouragement, this thesis would not be possible.

# CONTENTS

ABSTRACT.....	1
DECLARATION .....	2
DEDICATION .....	3
ACKNOWLEDGEMENTS .....	4
CONTENTS.....	5
ACRONYMS .....	7
LIST OF TABLES .....	8
LIST OF FIGURES .....	9
<b>Chapter 1 – INTRODUCTION .....</b>	<b>11</b>
1.1 Internet of Things .....	11
1.1.1 Coding Layer .....	12
1.1.2 Perception Layer .....	12
1.1.3 Network Layer .....	13
1.1.4 Middleware Layer .....	13
1.1.5 Application Layer .....	13
1.1.6 Business Layer .....	13
1.2 Radio Frequency Identification.....	<b>13</b>
1.3 Components of an IoT based RFID System.....	15
1.3.1 Internet Connection .....	15
1.3.2 RFID Reader .....	15
1.3.3 RFID Tag.....	15
1.3.4 Processing Unit .....	16
1.3.5 Storage Unit.....	16
1.4 Problem Statement .....	16
1.5 Objective .....	16
1.6 Areas of Application .....	17
1.7 Organization of Thesis .....	17
<b>Chapter 2 – LITERATURE REVIEW .....</b>	<b>18</b>
2.1 7-bit Chipless RFID tag with sensors .....	18

2.2	Chipless RFID Tag for Aviculture Industry .....	20
2.3	Chipless RFID Tag without Sensors .....	22
<b>Chapter 3 – Chipless RFID Tags .....</b>		<b>29</b>
3.1	Frequency Domain Reflectometry (FDR) Based Chipless RFID Tags .....	29
3.1.1	Retransmission Based FDR tags .....	29
3.1.2	Backscattering Based FDR Tags.....	30
3.1.2.1	Working of Backscattering Based FDR Tags .....	30
3.2	Proposed Tag Design .....	32
<b>Chapter 4 – RESULTS AND DISCUSSIONS .....</b>		<b>35</b>
4.1	TAG-A .....	36
4.2	TAG-B .....	36
4.3	TAG-C .....	37
4.4	TAG-D .....	38
4.5	TAG-E.....	39
4.5.1	Humidity Sensing.....	42
4.5.2	Experimental Setup for Humidity Sensing .....	44
4.6	Comparison with previous state of art tags .....	46
<b>Chapter 5 – CONCLUSION .....</b>		<b>47</b>
5.1	Future Work .....	47
<b>BIBLIOGRAPHY .....</b>		<b>50</b>



## ACRONYMS

RFID	Radio Frequency Identification
IoT	Internet Of Things
IR	Infrared
EM	Electromagnetic
FDR	Frequency Domain Reflectory
TDR	Time Domain Reflectory
RCS	Radar Cross Section
dbsm	Decibel per Square Meter
NLOS	Non-line of Sight
MWCNT	Microwave Carbon Nanotube
CO <sub>2</sub>	Carbon Dioxide
ML	Machine Learning

## **LIST OF TABLES**

3.1	Patch A and patch B measurements .....	33
4.1	Resonating frequencies of TAG-E.....	40
4.2	Tag's comparison with different substrates/laminates .....	42
4.3	Comparison with already presented tags .....	46

## LIST OF FIGURES

<b>Figure 1.1</b>	Six Layer Architecture of IoT.....	12
<b>Figure 1.2</b>	RFID System.....	14
<b>Figure 1.3</b>	IoT Based RFID System.....	15
<b>Figure 2.1.1</b>	Simulated response of temperature sensing.....	18
<b>Figure 2.1.1</b>	Measured cracked sensing response .....	19
<b>Figure 2.2.1</b>	22-bit Chipless RFID tag prototype.....	20
<b>Figure 2.2.2</b>	RCS response of 22-bit Chipless RFID Tag.....	21
<b>Figure 2.2.3</b>	Humidity sensing of the tag w.r.t X-probe .....	21
<b>Figure 2.2.4</b>	CO <sub>2</sub> sensing response of Tag.....	22
<b>Figure 2.3.1</b>	18-bit Chipless RFID Tag.....	23
<b>Figure 2.3.2</b>	RCS response with alternative bits .....	23
<b>Figure 2.3.3</b>	Flower shaped Chipless RFID Tag.....	24
<b>Figure 2.3.4</b>	RCS response of 12-bit Tag.....	25
<b>Figure 2.3.5</b>	First Tag design of 8-bits .....	26
<b>Figure 2.3.6</b>	RCS response of 1st tag design.....	26
<b>Figure 2.3.7</b>	Second tag design of 8-bits.....	27
<b>Figure 2.3.8</b>	RCS response of the second tag.....	28
<b>Figure 3.1</b>	Working Principle of Retransmission Based Tags .....	30
<b>Figure 3.2</b>	Patch A.....	34
<b>Figure 3.3</b>	Patch B.....	34
<b>Figure 3.4</b>	Presented Tag Design .....	34
<b>Figure 4.1</b>	Simulated result of Patch A .....	35
<b>Figure 4.2</b>	Simulated result of Patch B .....	35
<b>Figure 4.3</b>	Simulated result of TAG-A .....	36
<b>Figure 4.4</b>	Simulated result of TAG-B.....	37
<b>Figure 4.5</b>	Simulated result of TAG-C.....	37
<b>Figure 4.6</b>	Simulated result of TAG-D .....	38
<b>Figure 4.7</b>	Simulated result of TAG-E.....	39
<b>Figure 4.8</b>	Simulated response of TAG-E with unique Tag ID .....	41
<b>Figure 4.9</b>	TAG-E simulated response with alternate 1's Tag ID.....	41
<b>Figure 4.10</b>	Computed RH response using H-probe only .....	43

<b>Figure 4.11</b>	Computed RH response using H-probe only .....	43
<b>Figure 4.12</b>	Measured humidity sensing graph w.r.t H-probe .....	45
<b>Figure 4.13</b>	Measured humidity sensing graph w.r.t H-probe .....	45

# **INTRODUCTION**

In modern times, the internet has become an important tool for remote device control, data collecting and analysis, and information exchange. The Internet of Things is a term given to this technology commonly known as IoT. It is helping to improve our standards of life by transforming commonplace devices into far more intelligent ones [1-3]. A survey found that by the year 2025, the impact of IoT technology on our lives would be tremendous. It states that there will be 75 billion internet connected devices and IoT market will increase by the \$2.7 to \$6.2 trillion [4,5].

Radio Frequency Identification (RFID) fundamental concepts and IoT is explained briefly in this chapter. RFID is also an elementary building component of IoT. In some of the areas where RFID led IoT is considered as primary components will be discussed in this chapter. As we all know that IoT is taking over the market, sensor market is also exponentially rising. According to a survey, it is predicted that by the year 2041, sensor market will get the investment of almost \$250 billion [6]. These sensors are available in large varieties, which may be suitable for different sort of applications. By the year 2025, it is expected that per year revenue of wearable sensors may reach \$5 billion [7]. In some sort of applications printed sensors has taken over where these wearable sensors are suitable. By the end of 2030, it is expected that \$4.5 billion will be invested in printed sensor market [8]. To counter the problem of, aging of medicines, intelligent packaging was introduced. So, it is one of the reasons that intelligent packaging is gaining the popularity worldwide and it is estimated that intelligent packaging goods may reach \$895 billion by the year 2030 [9]. This gives us the motivation to work on Chipless RFID tags to replace those conventional and expensive sensors with economical Chipless RFID tags-based sensors.

### **1.1 Internet of Things**

IoT is basically a network of interconnected devices, which communicate with each other and with the cloud as well without human intervention. It is evolving continuously and currently the hot research topic because of its infinite opportunities. It's an approach of collecting and sending data to any virtual platform after getting it

from different kind of things [10]. IoT allows the exchange of information between imperceptible things by using the technology of RFID [11]. Generally, an IoT system or architecture can be divided into six layers [12] as shown in Fig.1.1.

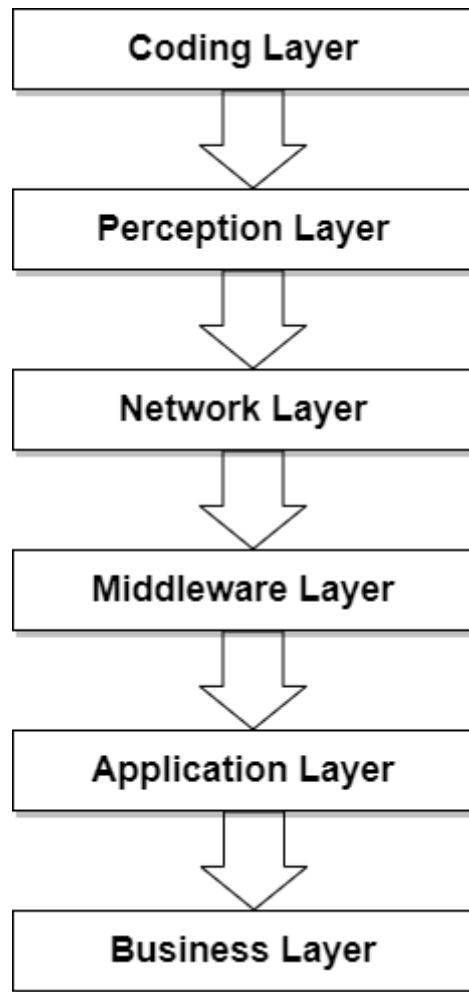


Fig.1.1 Six Layer Architecture of IoT

Here is the brief introduction of all the six layers.

### **1.1.1 Coding Layer**

This layer, which makes use of technologies like RFID to designate each object of interest with an individually unique identification ID, is regarded as the IoT's foundation [13].

### **1.1.2 Perception Layer**

Purpose of this layer is to give physical meaning to the object of interest by utilizing the different type of sensors like Infrared Sensors (IR) sensors, RFID tag-based

sensors which may sense temperature, crack, humidity of objects [14]. So, this layer collects the information from different sensors, convert this information into the form of digital signals and then forward these digital signals to network layer for further processing.

### **1.1.3 Network Layer**

This layer transmits the information, which was gathered in the form of digital signals, to the middleware layer by making the use of commonly known technologies like Bluetooth, Wi-Fi, Zigbee etc.[15].

### **1.1.4 Middleware Layer**

This layer makes use of the data from the network layer and makes sure that all relevant data can be accessed from databases. It makes use of ubiquitous computing and cloud computing tools [11].

### **1.1.5 Application Layer**

The purpose behind this layer is to apprehend the practice of IoT in all kinds of industries, because an application is the best way to promote the IoT in large scale industries. These applications may include smart homes and smart transportation etc [16].

### **1.1.6 Business Layer**

This layer is responsible for managing the services and the research that is being carried out related to IoT by recommending the different business strategies [17].

## **1.2 Radio Frequency Identification**

The RFID technology is the fundamental enabler for IoT technology. Because this technology works on coding and perception layer of IoT, as it's playing key role in the identification and tracking technologies [18]. According to a survey mentioned in [19], In 2030, the RFID market is anticipated to surpass USD 35.6 billion. Due to the adaptability of information technologies RFID is providing the modern solution to industrial and consumer applications. RFID basically uses electromagnetic waves (EM) waves for the identification of a particular object. An RFID reader transmits an interrogation signal to an RFID tag, then it gathers the reflected signal from the tag that contains the encoded data. Later, this reflected signal is decoded to retrieve the

required information by using the different algorithms [20]. So, in this all scenario, RFID tag is a very crucial component, because it is used to get the information from the environment, on which all the actions are dependent. In Fig.1.2, a typical RFID system is displayed. Our focus of research is tags. So, we will discuss about tags in detail later.

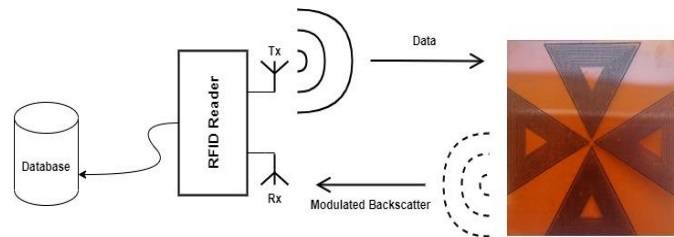


Fig.1.2. RFID System

### 1.3 Components of an IoT Based RFID System

An IoT based RFID system consists of various constituents, in which each perform its own allocated task [21]. As each node perform its own task in this smart environment, so it's basically the collective effort of each node. The devices in this environment react to ongoing events based on their integrated intelligence. Some efforts and finance are required to build up a system, but later on once system is established, intelligence devices take on. Figure 1.3 shows the some of the components of an IoT based RFID system. RFID technology is utilized for the interconnectivity of the devices. In RFID a unique number is assigned to each device in the network for communication. RF waves are used for the transfer of information from one device to another in the wireless communication [22].

The primary components of the network are almost same, but the secondary components may differ, it depends on the environment for which the network is being designed. Here we will discuss the function of primary components of the network.



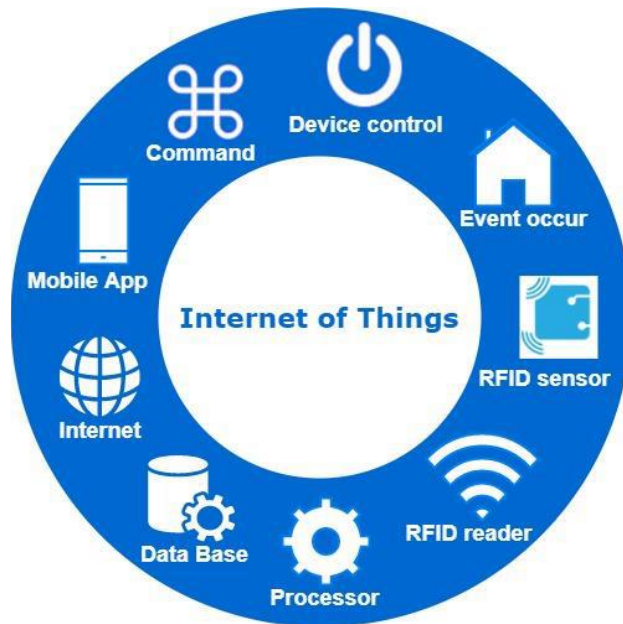


Fig.1.3 IoT Based RFID System

### 1.3.1 Internet Connection

Internet itself is the key part of IoT technology [23]. It plays a key role to form a giant network by the interconnection of small networks. To route all information over the cloud and to access the information to the authorized persons internet connection is unavoidable.

### 1.3.2 RFID Reader

RFID reader is used to get the information from the tags by sending and receiving the RF waves because they have the transmitting and receiving antennas. It works on specified frequency band depending on the type of application.

### 1.3.3 RFID Tag

Basic building block of this network is the RFID tag that stores the information in the form of bits. When the interrogation signal hits this tinny node, it reflects the encoded information which is collected by the reader [24]. The RFID tags can be active, semi-passive, or passive in nature. The choice of the RFID tag is made in any application depend on the requirement [25]. Active tags may send the information up to approximately 100 feet because they have their own transmitting and receiving antennas along with the power source . Passive tags don't contain any battery source as compared to semi passive tags which may contain the battery source. Reflected or backscattered signals of passive tag depend on properties of the tag [26]. Passive tags consist of

resonating structures only and any change in the substrate properties yields an alteration in the reflected frequency domain reflectory (FDR) response of the RFID tag. As the RFID reader collects the backscattered signal, an algorithm is used to decode the signal.

#### **1.3.4 Processing Unit**

This part required different for the targeted applications to introduce the intelligence in the system. The compatibility of the processing unit with the rest of the system requires complex programming techniques [27]. This processing unit decodes the information received from the reader and compare the received information with the previously stored information and forward the commands to the owner based on the algorithm.

#### **1.3.5 Storage Unit**

Every bit of information routed over the network is stored in the database [28]. For monitoring purpose, time to time values is required which can be taken from database. For comparison in daily routine monitoring tasks, several days values are required which can be stored in database. These values are accessible from anywhere in the world at any time. For ongoing situation in the network these recorded values play a very key role in creating solution.

### **1.4 Problem Statement**

RFID is playing a key role in transforming the conventional devices into smarter ones by providing the physical data in real time. Chipless RFID is gaining the attention because of its low-cost, better-read range, flexibility, reliability than conventional technologies like barcodes. To make it more cost effective it is more suitable to use a material which also act as a sensor along with tagging the multiple items.

### **1.5 Objectives**

The aim of this research is to enhance the productivity and efficiency of the chipless RFID tag. The objective of this research is to design an RFID tag that can facilitate the customer in every field of life. Regardless of the cost and manufacturing complexities, these chipless tags should be vastly available to opt for without any hesitation. Following are the objectives of this research

- ✓ To realize the unique design chipless RFID tag that offer multiple items tagging with low cost

- ✓ To realize the chipless RFID on different materials or substrates to use the tag in different environmental conditions
- ✓ To make the use of material that also offers sensitivity along with tagging items
- ✓ To ensure the printability of the tag, so that mass production could be possible
- ✓ To ensure the flexibility of the tag, so that tag can be used on irregular surfaces
- ✓ To make the use of efficient band utilization, so that multiple bits can be achieved with less frequency band

## **1.6 Areas of Application**

Chipless RFID tags are the primary components of IoT as mentioned earlier. These chipless RFID tags can be used in pharmaceutical industry to track the record of medicines and to monitor the humidity and temperature of drugs so that drugs don't become hazardous for health. Chipless RFID sensors plays a significant role in food safety, the attached sensors may help the supplier to monitor their products in the retail chain, the CO<sub>2</sub> concentration in the fruit can be detected even though the product looks fine from outside [29-30]. Overall, the chipless RFID tags providing its mind-blowing services in health monitoring , smart homes, aviculture industry and many more [31-33].

## **1.7 Organization of Thesis**

Brief introduction of thesis is summarized in Chapter 1. Chapter 2 presents the literature review on Chipless RFID tags. Chapter 3 provides the details on the types of RFID tags. Chapter 4 demonstrates the results and discussions of the proposed work. Proposed work is concluded in chapter 5 along with the future work.

## LITERATURE REVIEW

Chipless RFID tags is a very vast field but the working principle of almost every tag is same. The differences are made based on the number of encoding bits, frequency band utilization and sensing etc. The chipless RFID tags have been the subject of profound research. In this chapter we will discuss some of the research that has been carried on the chipless RFID tags of our interest.

### 2.1 7-bit Chipless RFID Tag with Sensor

A chipless RFID tag is presented in Ref [33]. This research introduces small, 7-bit chipless, multiparameter RFID sensor made of sophisticated Rogers RT/Duroid® 6010.2LM laminate. When temperatures change, the material's dielectric characteristics change. Six resonators having inverted "U" and "L" shapes with appropriate dimension have been designed to resonate within the frequency range of 2-8 GHz. A circular patch antenna is used to analyze the crack. The measurements are carried out in a space that is electromagnetically quiet outside of the anechoic chamber. The developed new intelligent sensor can be used to track any metal

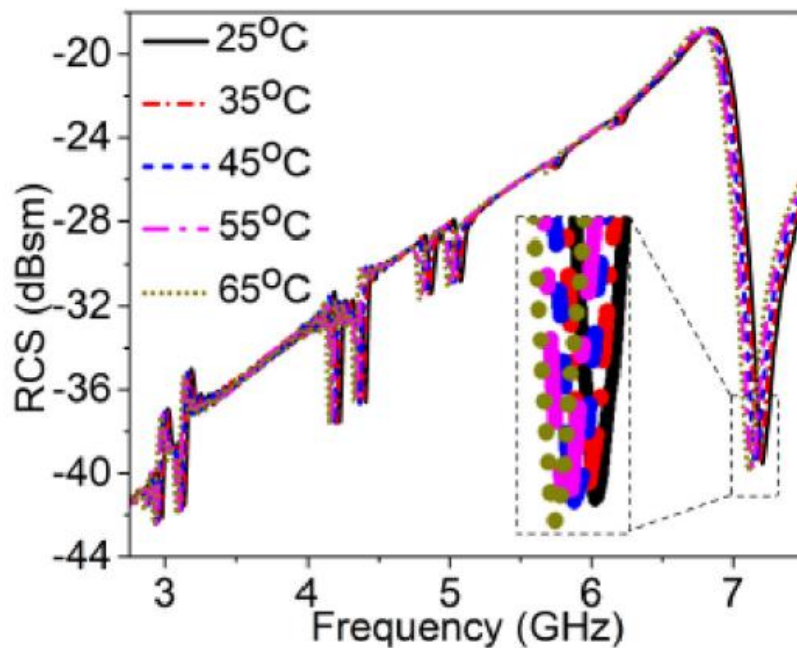


Fig 2.1.1 Simulated response of temperature sensing

surface cracks, where temperature control is also important. The cutting-edge robust multisensor that is being presented is appropriate for long-term applications. Figure 2.1.1 shows the temperature sensing of the tag because the substrate used shows the drift in frequency when exposed to changing temperature. Here we can clearly see the shift towards the left side because relative permittivity of the substrate increases when temperature increases due to which the response shift towards the lower frequencies. Similarly for crack monitoring CMPA is used. For that reason, two metallic samples are individually linked to the specified chipless sensor. DuPont TM Pyralux® LF sheet adhesive was employed to attach metallic samples to the realised sensor. Using several metallic plates that are cracked, the RCS response of the tag is measured. It is observed that a case with a broader crack generates a notch that is not as deep. If the metallic framework cracks, more air particles may enter the gap. The surface current is disrupted by these air particles, and as a result, the frequency notches gradually change and shift. A larger crack will therefore eventually have a lower current density, which will lead to a weaker response notch. The observed measured frequency graph for two samples, displayed in Figure 2.1.2, clearly demonstrates this effect. A crack in sample 1 is around 0.5 mm broad, but a crack in sample 2 is only 0.1 mm wide. According to the simulations' findings, the crack detection sensitivity is  $f_r = 58.8$  MHz shift and 0.358 dB amplitude degradation of a CMPA resonance for every 0.1 mm increase in fracture width. The resonances of the other resonators

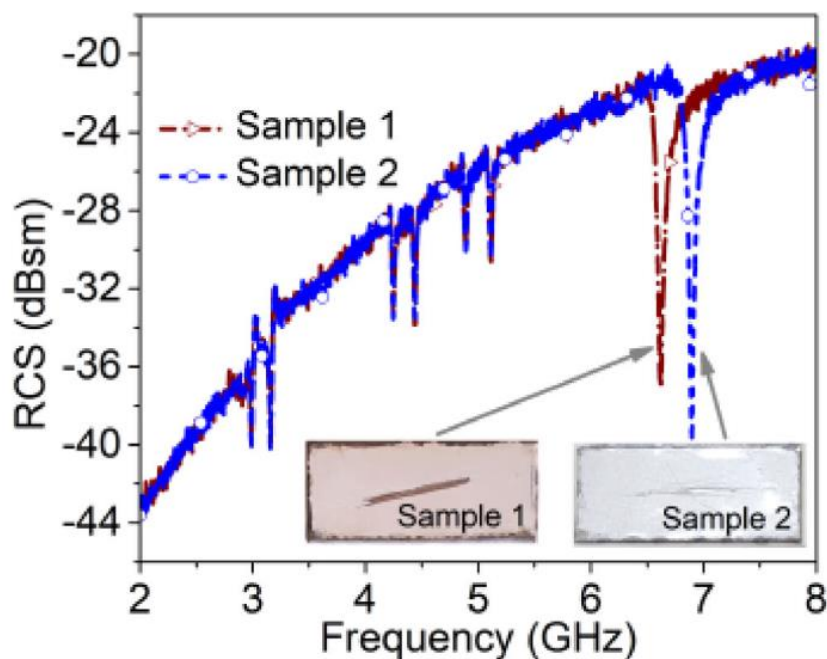


Fig. 2.1.2 Measured crack sensing response

show no discernible change. In this instance, the tag functions as a 6-bit tag with six identification resonances and one resonance for crack sensing.

## 2.2 Chipless RFID Tag for Aviculture Industry

In Ref [33], CST Studio Suite is used to create and simulate a 22-bit chipless RFID tag, as seen in Figure 2.2.1. It has a copper radiator-like patch in the shape of a circle over the substrate. By adding slits to the design, 11 circular slots on the radiator are further divided into 22 c-shaped slots. Each slot is built with a variable length due to the slit S2, which causes each slot to vibrate at a distinct frequency. Therefore, higher data density by doubling the frequency notches is achieved.

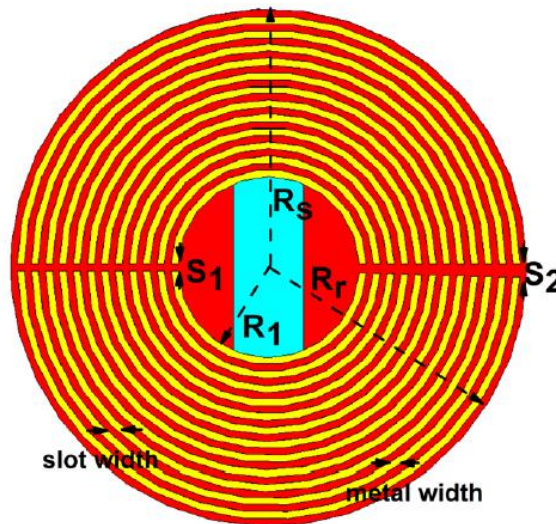


Fig 2.2.1 22-bit Chipless RFID tag prototype

Dual-polarized antennas are used to interrogate tags instead of circularly polarized ones because of the tags' dense frequency response. The response of a Kapton HN-based tag is shown in Figure 2.2.2 as horizontally and vertically polarized plane waves. Since each slot corresponds to one bit, a tag structure has 22 frequency dips in the required frequency spectrum. A dip represents the first logical condition, "1". The tag ID for a tag with 22 slots will therefore include 22 1s, or 11111111111111111111. By shorting or eliminating the slots from the given tag, several tag IDs can be created. Because of small shifting and changing in the depth, this shortening of the slot has very little impact on nearby notches. The tag utilizes a bandwidth of almost 19 GHz.



When subjected to varying moisture levels, the Kapton®HN substrate's electrical characteristics alter. During this experiment, this impact is seen by sprinkling water into the airtight climatic chamber. The RCS response has been achieved after the lid has been closed for 10 minutes. As the chamber's relative humidity (RH) level

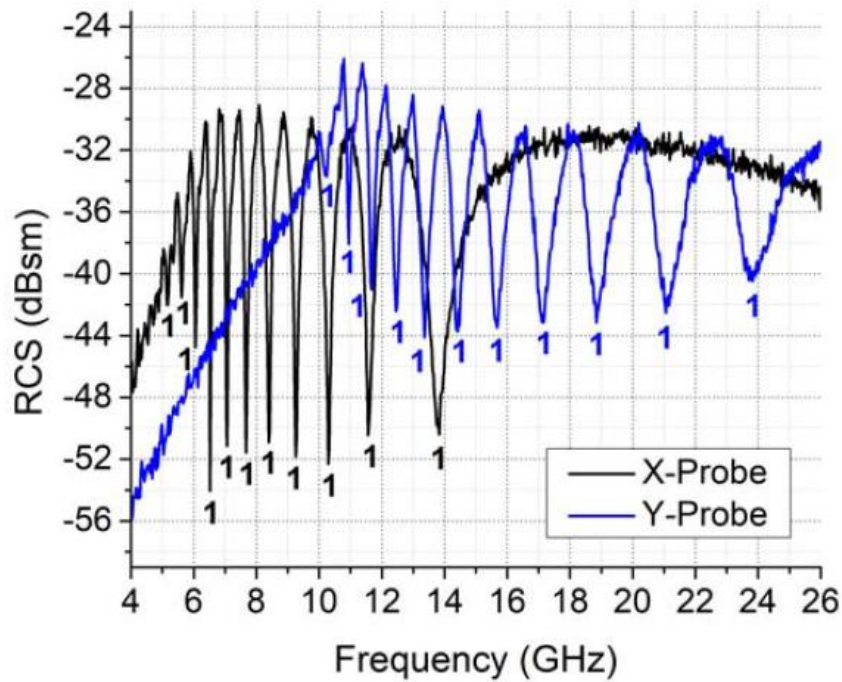


Fig. 2.2.2 RCS response of 22-bit chipless RFID tag

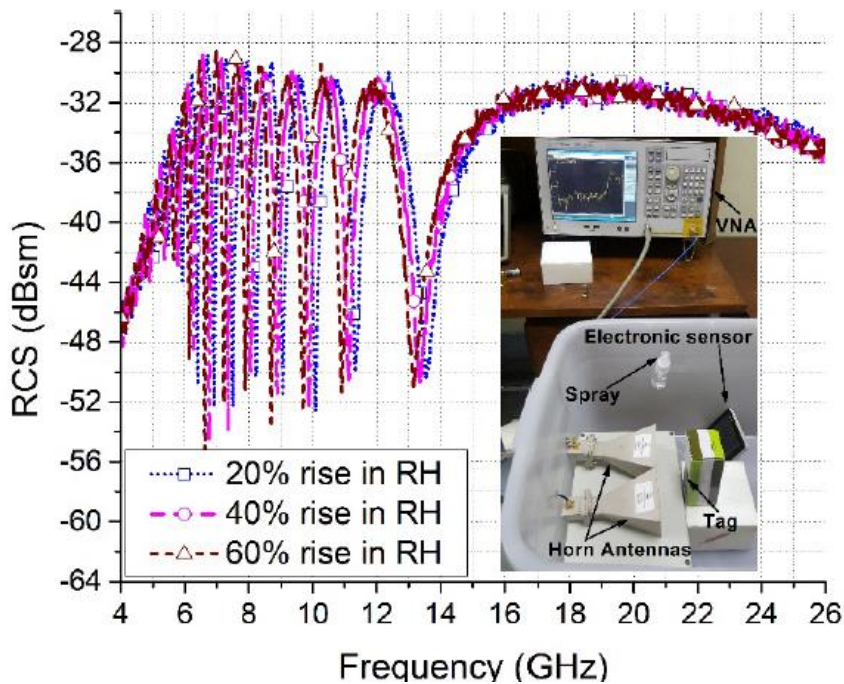


Fig. 2.2.3 Humidity sensing of tag w.r.t X--probe

Increases, frequency band moves towards lower frequencies because of water which is sprayed inside the chamber as shown in Figure 2.2.3. When the cover is lifted, the RH level drops back to room temperature and the chipless sensor goes back to its initial configuration. As illustrated in Figure 2.2.4, the suggested multiparameter sensor is put to the test for CO<sub>2</sub> sensing once MWCNT is incorporated into the finished design. After MWCNT is deposited at room temperature, the required response of the innermost slot is significantly reduced by 10 dBsm. The previously created airtight chamber is fitted with the multisensor, and 20 000 ppm CO<sub>2</sub> gas is then introduced. The CO<sub>2</sub> gas is first absorbed by the MWCNT that has been placed over the tag. The amount of CO<sub>2</sub> gas absorbed is inversely correlated with the amount of CO<sub>2</sub> in the chamber and directly proportional to MWCNT resistivity.

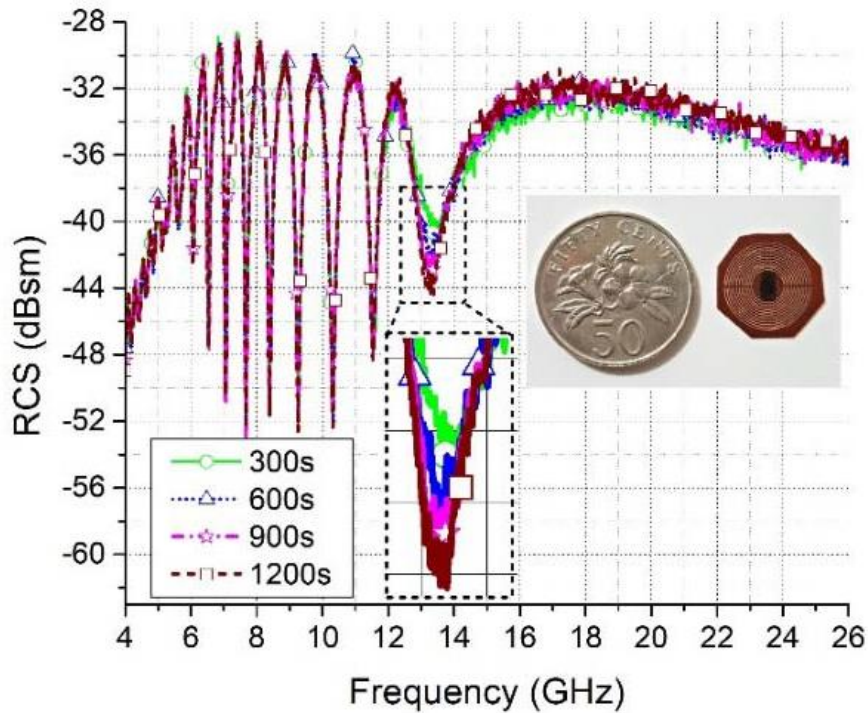


Fig. 2.2.4 CO<sub>2</sub> sensing response of the tag

### 2.3 Chipless RFID Tags without sensors

An innovative printable chipless RFID tag design concept for small objects is presented [36]. The tag is made up of a triangle-shaped patch that is filled with several triangular shaped slot resonators. The same patches are duplicated six times and put together to create an extremely small, long-range chipless RFID tag. Both a near-field and a far-field chipless RFID tag reader are capable of reading the tag. Figure 2.3.1



shows the Chipless RFID tag design made up of 6-patches arranged in hexagonal manner.

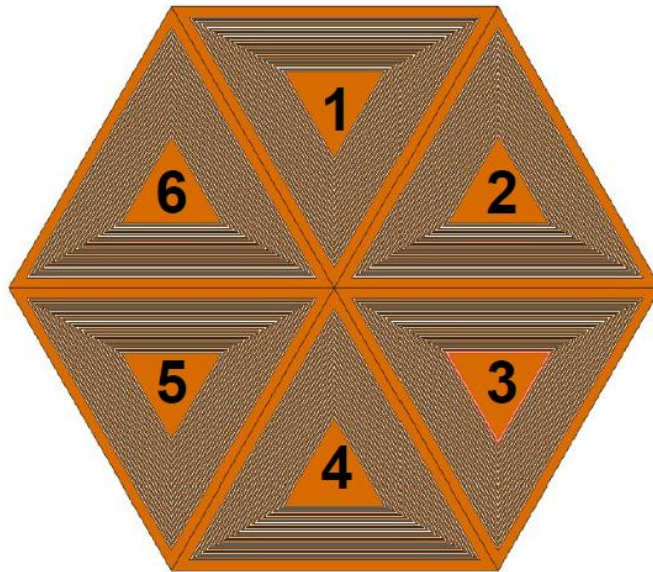


Figure 2.3.1 18-bit Chipless RFID tag

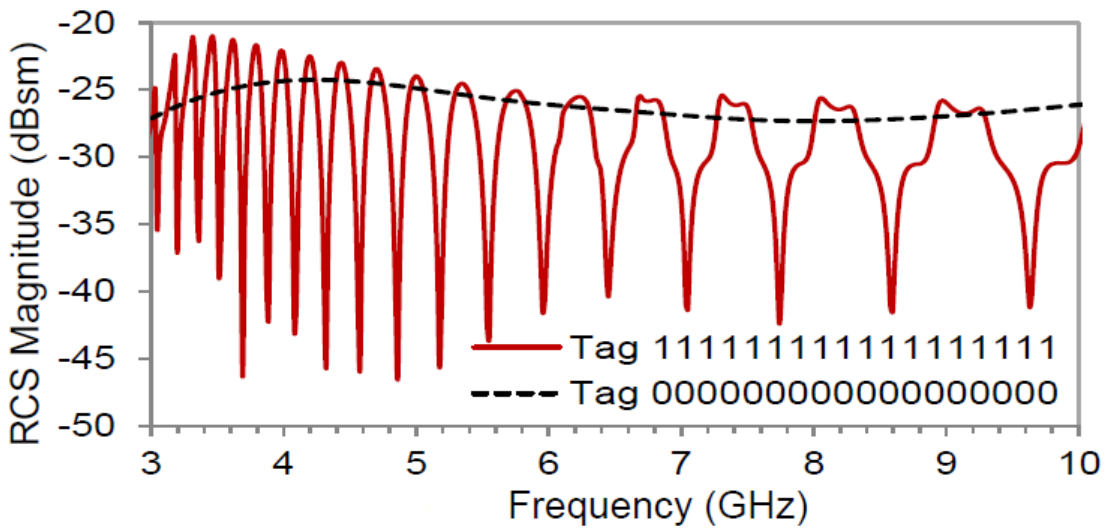


Fig. 2.3.2 RCS response with alternative bits

Fig.2.3.2 shows the simulated response of the tag having all 1's and all 0's which means the tag is able to encode  $2^{18}$  bits. A minor shift is observed in simulated response while generating different encoding bits but this shift can be overcome by using signal processing. A Quick Response (QR)-based having 110 bits data encoding capacity Chipless RFID tag is introduced in [35]. An RT/Duroid® 5880 without

ground plan is used as substrate over the area of  $5.5\text{cm}^2$ . In these 110 bits, 102 bits are achieved through optical domain and only 8 bits are achieved through spectral domain. As the optical and spectral domain are used at same time, so mentioned tag has complex labeling and reading method. Also, for QR-based encoded bits Line of Sight (LOS) is required. Another tag is presented in [37]. This study examines a polarization-independent, fully printed, frequency-coded chipless RFID tag in the flower like shape. The tag has a 12-bit data encoding capacity. As a frequency signature of the resonators, RF encoding particles are used to encode and transmit the data. The 8 to 11.5 GHz spectrum is covered by the 12-bit tag that is being proposed. The software CST Microwave Studio is used to simulate and design the tag. The simulation is performed on a FR-4 low-cost substrate with a tangent loss of 0.018 and a 4.3 dielectric constant value. Due to its small size (13 mm x 9 mm), this compact tag can be inexpensively printed on substrates with one side.

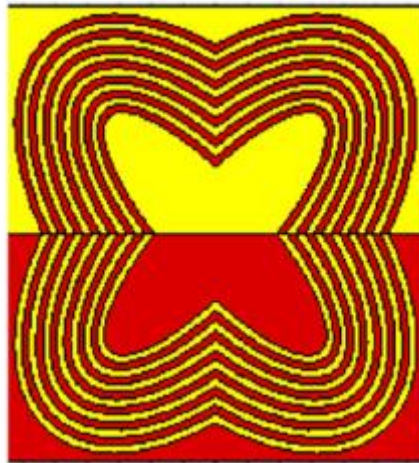


Fig. 2.3.3 Flower shaped chipless RFID tag

Figure 2.3.3 shows the flower shaped tag design and Figure 2.3.4 shows the RCS response of the tag which indicates the 12-bits means that the tag has the capacity of encode 4096 objects. . Similarly, another Chipless RFID is presented in reference [38] having the data encoding capacity of 6-bits based on FDR. Overall, 0.5 GHz BW is

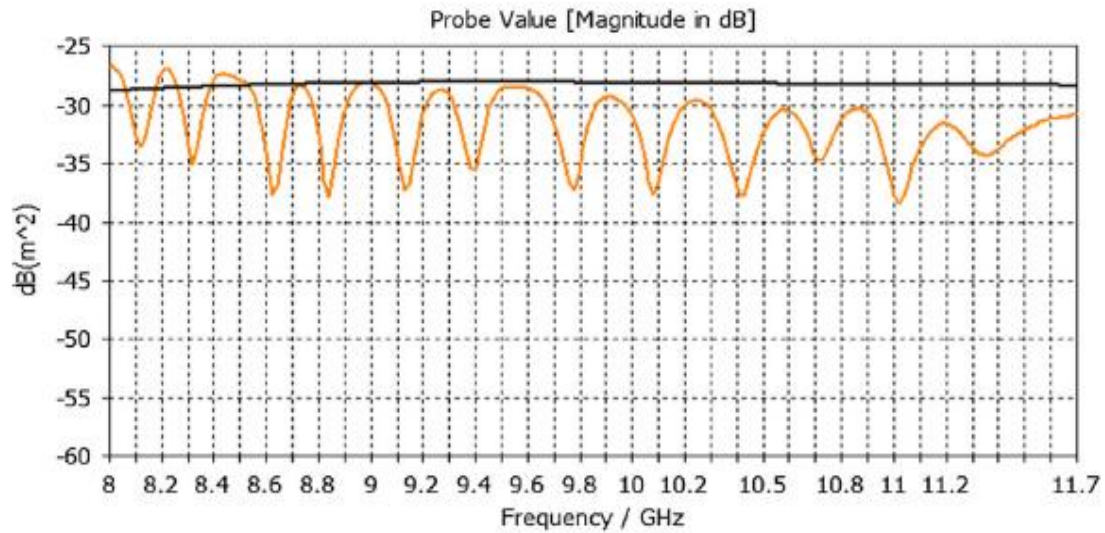


Fig. 2.3 4 RCS response of 12-bit tag

is utilized in this referred paper and is realized over the span area of  $3.313 \times 1.225 \text{ cm}^2$ . This tag which contains the multi-resonators exhibits the bit density of  $1.771 \text{ bits/cm}^2$ . Also, a rigid laminate TLX-8 is employed as substrate and for radiating purpose copper is used.

This tag can't be applied on irregular surfaces. For IoT applications like identification, tracking this tag can be utilized. A 16-bit FDR based Chipless RFID tag having the area of  $15 \times 20 \text{ mm}^2$  is presented in reference [39]. It has the bit density of almost  $5.08 \text{ bits/cm}^2$ , and it's designed over the Rogers RO4003, which is a rigid substrate. Radar Cross Section is used to analyze the behavior of the tag and it doesn't possess any sensing capability. Two innovative small orientation independent chipless RFID tags are shown, together with their designs, for new applications like the internet of things in Ref [40]. These tags generate resonances in the backscattered radar cross-section spectrum when they get subjected to RF waves, and those waves are then used to encode the data. These have their basis on L-type resonators, which lack a ground plane and may wade through from the back and front side using linear polarization waves. L-resonators are positioned in the lower triangle of the substrate in the first tag design which increases mutual coupling, but size is reduced here. In the second tag design, which has a lower mutual coupling and better printing strength but a lower bit density, alternate L-resonators are employed in both halves of the substrate. The presented idea is illustrated with 8-bit chipless tag prototypes using Rogers substrate. These tags have a compact  $20 \text{ mm} \times 20 \text{ mm}$  board size and a very low bandwidth

requirement for 8-bit encoding. Figure 2.3.5 shows the first tag design and Figure 2.3.6 shows the RCS response of that first tag design.

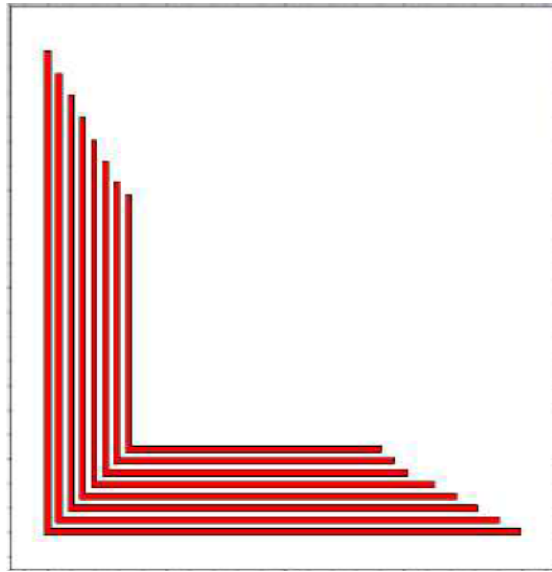


Fig. 2.3.5 First Tag design of 8-bits

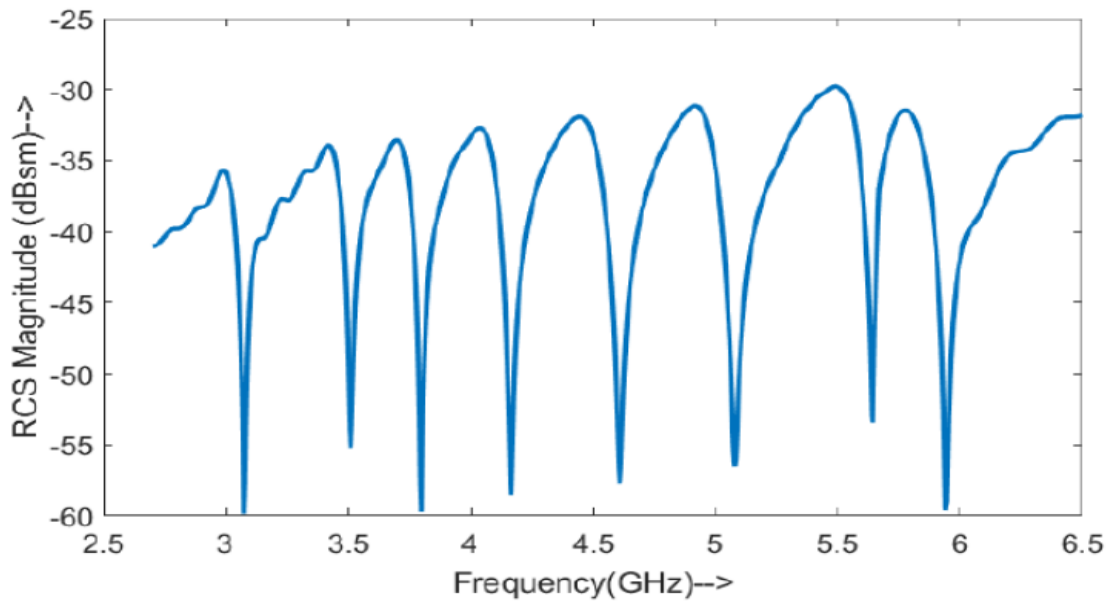


Figure 2.3.6 RCS response of 1st tag design

The most significant bit of the encoded data is assigned to the longest resonator, while the least important bit is assigned to the smallest resonator. A "1" will be used to indicate the presence of a frequency signature, and a "0" to indicate its absence. The resonator-based chipless tag resembles a wideband antenna in its behavior. The advent

of more sophisticated printing technologies can make it possible to incorporate more resonators and, as a result, encode more bits without growing the tag's size. In any

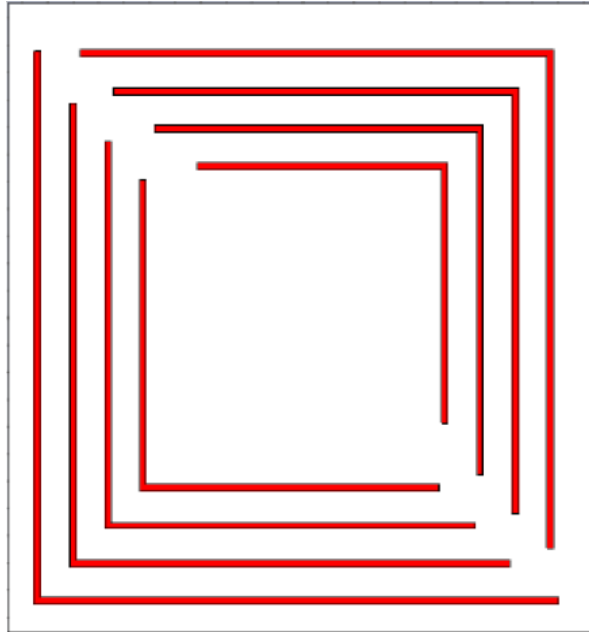


Figure 2.3.7 Second tag design of 8-bits

case, the size will linearly not increase with the increasing number of bits. The tag size for the 8-bit example is 20 mm x 20 mm, which easily satisfies the demand for small tags for IoT applications. The closeness of the resonators to one another in this design, however, can reduce overall performance because of mutual coupling, that can cause issues with the accurate reading of the tag. Its scalability appears to be another drawback. Figure 2.3.7 shows an alternative design for a collection of frequencies related to the first idea. The odd-numbered resonators are in the bottom triangular side of the design, while the even-numbered resonators are in the top triangular side. Once more, the lowest frequency in the tag gets assigned to the longest resonator, while the highest frequency happens to be generated by the shortest resonator. Figure 2.3.8 shows the RCS results of the second tag design. This study has presented new designs for two orientations independent chipless RFID tags that perform noticeably better than the existing versions. The arrangement of the L-resonators correctly results in the designs' inherent orientation independence. Interesting attributes of the recommended tags include printability, low bandwidth, high bit density, short size, and front- and back-readability in addition to orientation independency. These attributes have all been examined in simulation and put to the test empirically. Additionally, if some

characteristics can be traded off, the designs have been demonstrated to have potential as cost-effective mass deployment options.

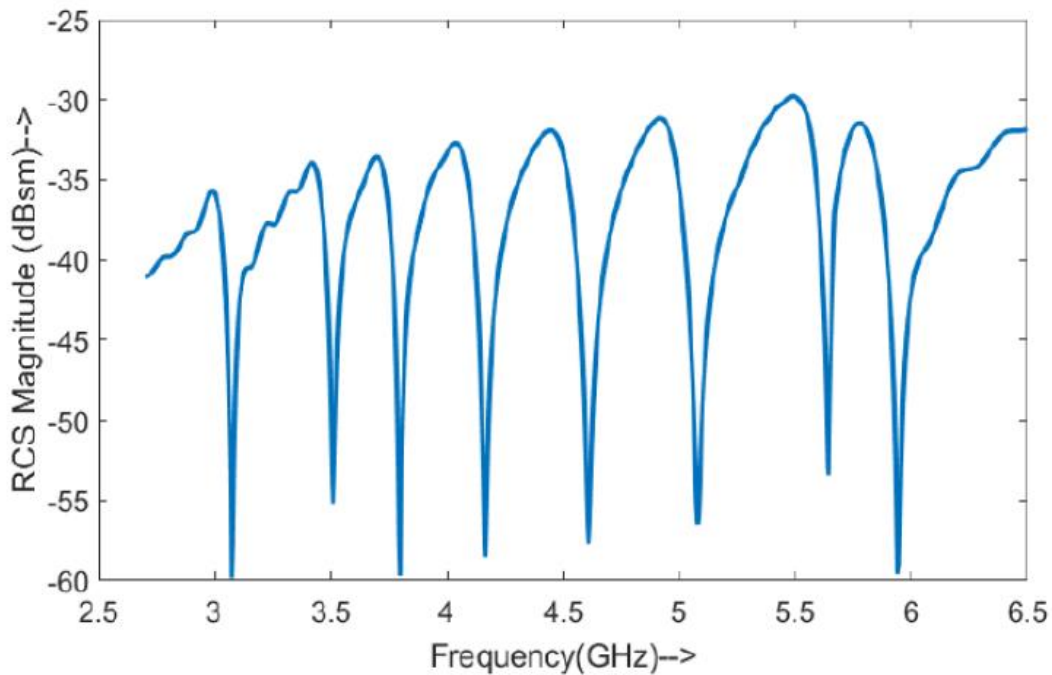


Fig. 2.3.8 RCS response of the second tag

In [41] an elliptical shaped orientation independent Chipless RFID tag is presented which has the encoding capacity of 10 bits. It works in the frequency domain of 3.6 to 15.6 GHz and to energize the tag linear polarization-based RF wave is used. The tag utilizes the bandwidth of 12 GHz, so it has the spectral density of 0.83 bits/GHz. To analyze the behavior of the tag RCS response is used. This referred tag is analyzed on the different substrates like Rogers RT/Duroid/5880, Rogers RT/Duroid/5870 and TLX-0 to use the in different environmental conditions. The framed structure functions in the 3.6 to 15.6 GHz RF spectrum, and different encoding bit combinations are made possible by adding and removing slots. The Rogers RT/duroid/5880 substrate provides the flexibility, and the tag's polarisation insensitivity allows it to operate across a range of oblique angles from 00 to 600. In order to authenticate and identify millions of objects, this tag is a viable candidate to be installed on uneven surfaces. Similarly, another green electronics based chipless RFID tag is presented in reference [3]. This referred tag is analyzed on a paper substrate and it possesses the encoding capacity of 12-bits which means it can be used to tag the  $2^{12}$  items. For sensing purpose carbon nano tube is used in the center of the tag to sense the gas. To analyze the behavior of the tag RCS response is used.

### **Chipless RFID Tags**

RFID tags are categorized into chip-based RFID tags and chipless RFID tags. Chipped tags are those tags, which contain the silicon chip and data is stored in that chip. Chipless tags are those tags which contain the resonating structure only. Although chipped tags have long read range and data storage capacity, but they are more expensive and rigid that's why our topic of interest is chipless RFID tags because of flexibility, less expensive and more reading range than conventional technologies like barcodes. We will discuss chipless RFID tags and their types in detail in this chapter. Chipless RFID tags can be divided into different types based on the encoding techniques. These chipless RFID tags can be divided into time domain [43], frequency domain [44], image based [45] and hybrid chipless RFID tags [46]. Till now better response is achieved by frequency domain reflectometry-based tags as in which each specific frequency is depicted by corresponding bit [47].

#### **3.1 Frequency Domain Reflectometry (FDR) Based Chipless RFID Tags**

FDR based chipless RFID tags are those tags in which each bit has a unique frequency to represent it. They can be also categorized on two groups based on orientation of transmitted and reflected named as co-polar and cross polar tags. Co-polar means that the orientation of transmitted and reflected wave is same and cross-polar means that the orientation of transmitted and reflected wave is perpendicular to each other. Furthermore, FDR based tags can be retransmission-based tags and backscattering-based tags.

##### **3.1.1 Retransmission based Chipless FDR tags**

Retransmission based Chipless RFID tags are those tags which contain both the transmitting and receiving antennas along with the resonating structure. Figure 3.1

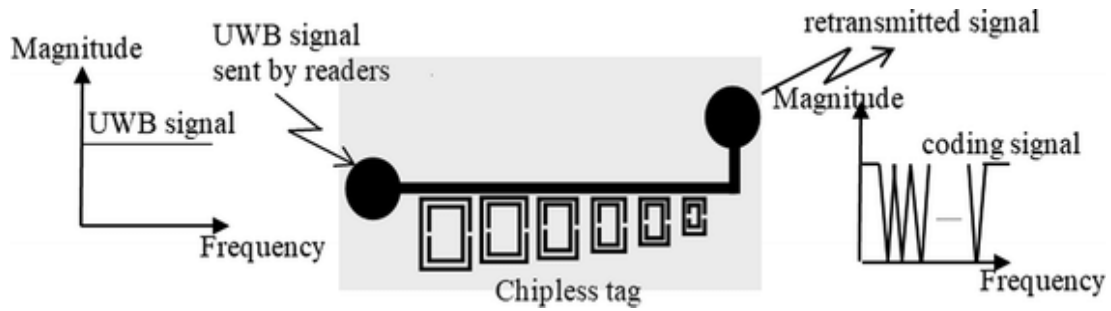


Fig 3.1. Working Principle of Retransmission Based Tags

shows the retransmission-based chipless RFID tags' operating system. The receiving antenna of the tag collects the signal transmitted from the reader antenna and pass it to the resonating structure of the tag which convert it to the distinct frequency signatures and this coded signal is then transferred to the transmitting antenna of the tag. Transmitting antenna of the tag passes this coding signal to receiving antenna of the tag which is then decoded to retrieve the information. As these tags contain the transmitting and receiving antenna therefore their size and cost increases.

### 3.1.2 Backscattering based Chipless FDR tags

Backscattering based Chipless FDR tags are those tags which contain the resonating structure only. Like retransmission-based tags it does not contain any transmitting and receiving antenna. Figure 1.2 shows the working principle of backscattering based chipless RFID tags. As our topic of interest is backscattering based chipless RFID tags, therefore we will discuss in detail.

#### 3.1.2.1 Working principle of Backscattering based Chipless FDR tags

A localhost-running database, tag, and reader make up a chipless RFID system. The reader emits RF energy into the surrounding environment in the direction of the tag, which causes the tag to behave like a radar target with a distinct electromagnetic signature used for coding Chipless RFID tags. Equation (1) can be used to determine the incident signal's power[48].



$$\frac{P_{RX}}{P_{TX}} = \left(\frac{\lambda}{4r\pi}\right)^2 G_{TX}G_{RX} \quad (1)$$

Where  $r$  is the distance between the tag and the reader,  $P_{TX}$  and  $G_{TX}$  are the power and gain of the transmitter,  $P_{RX}$  and  $G_{RX}$ , respectively,  $P_{TX}$  and  $G_{TX}$  are the power and gain of the receiver and denote the wavelength. This power which originates out of the incident signal by the tag, induces a current distribution inside the tag. In the form of an encoded wave, the tag radiates electrical power back towards the reader. Backscatter is the term for this power that is reflected to the reader[34], this phenomenon is portrayed in Figure 1.2. The reader decodes the distinctive tag ID using the backscattered signal to identify the remotely placed items. Physical EM signatures are used to encrypt the tag ID because chipless RFID tags do not have memory. These signals are modulated by the tag's resonating structure [49]. Either in the time domain or the frequency domain, the reader modulates the query signal. The bit density for time-modulated tags is very low [50] i.e., a big tag size can be used to encode a few bits. Frequency modulation-based tags, which offer better data density, are used to get around the time modulation-based tags' restriction. The resonant components in the tags used in frequency-domain RFID systems are tuned to different frequencies. Equation (2) provides the resonance frequency of each dip that correlates to the slot.

$$f_r = \frac{c}{2L} \sqrt{\frac{1}{\epsilon_r}} - 2\Delta L \quad (2)$$

Where  $\epsilon_r$  indicates the relative permittivity of the substrate,  $L$  symbolize the length of the slot,  $\Delta L$  arises due to effective dielectric constant [51]. 1-bit coding is indicated by the presence of resonance at the particular frequency. The Radar Cross-Section (RCS) of the tag provides the distinct frequency signature in the desired frequency band [2, 52]. Analysis of the tag's RCS response at Fraunhofer far-field distance is carried out through eq (3)[53].

$$R = \frac{2D^2}{\lambda} \quad (3)$$

Where  $\lambda$  is the wavelength of the incident wave and  $D$  indicates the largest dimension of the tag.

### 3.2 Proposed Tag Design

In this research work a 55.3 55.3 mm<sup>2</sup>-sized having encoding capacity of 2<sup>30</sup> bits is presented. As seen in Figures 3.2 and 3.3, the presented tag is made up of two different resonators length patches called "Patch A" and "Patch B." Both pair feature slots and resonators in the opposite positions, which causes the slots on one patch to resonate at a different frequency than the resonator/slot on the other patch. As seen in Figure 3.4, both patches are placed in a star-like pattern to enable the tag ideal for higher read range. On vertical axis, a pair of Patch A is placed, and on horizontal axis pair of Patch B is placed. The overall dimensions/area of both patches are the same at 31.35mm<sup>2</sup>. For the higher depth resonating dips, some slots and resonating structures of patches are employed at different widths which range from 0.2mm to 0.6mm as shown in Table 3.1. To make the tag suitable for printing when employing the active ink which here is silver nano ink, the lowest slot width of the tag is kept at 0.2mm. Table 3.1 displays the dimensions of the radiators and slots for Patch A and Patch B respectively.  $S_{ij}$  denotes the patch  $j$  ith slot, i.e.,  $S_{1A}$  denotes the patch A first slot. Similarly,  $M_{ij}$  designates patch  $J$  ith metal/radiator. The tag response remains same along the orthogonal axis because some of its slots are energized by an y-polarized plane wave while some are energized by a x-polarized plane wave. Each slot correlates to one notch or dip when the EM wave hits the tag structure [6]. Resonating dips are marked with a "1" when they are present and a "0" when they are not. Every patch has the ability to encode the 15-bit data because each patch has 15 slots, hence the tag is in charge of encoding a total of maximum 30 bits of data. CST MICROWAVE STUDIO® (CST-MWS) is tool in which tag is designed, tested, and optimized. The tag is excited using a dual-polarized wave which is already mentioned earlier.

Patch A			Patch B		
Radiator/Slots	Length	Width	Radiator/Slots	Length	Width
M1A	31.35mm	0.3mm	M1B	31.35mm	0.6mm
S1A	30.31mm	0.3mm	S1B	29.27mm	0.3mm
M2A	29.27mm	0.3mm	M2B	28.23mm	0.3mm
S2A	28.23mm	0.3mm	S2B	27.19mm	0.2mm
M3A	27.19mm	0.2mm	M3B	26.50mm	0.2mm
S3A	26.50mm	0.2mm	S3B	25.81mm	0.2mm
M4A	25.81mm	0.2mm	M4B	25.11mm	0.2mm
S4A	25.11mm	0.2mm	S4B	24.42mm	0.2mm
M5A	24.42mm	0.2mm	M5B	23.73mm	0.2mm
S5A	23.73mm	0.2mm	S5B	23.04mm	0.2mm
M6A	23.04mm	0.2mm	M6B	22.34mm	0.2mm
S6A	22.34mm	0.2mm	S6B	21.65mm	0.2mm
M7A	21.65mm	0.2mm	M7B	20.96mm	0.2mm
S7A	20.96mm	0.2mm	S7B	20.26mm	0.2mm
M8A	20.26mm	0.2mm	M8B	19.57mm	0.2mm
S8A	19.57mm	0.2mm	S8B	18.88mm	0.2mm
M9A	18.88mm	0.2mm	M9B	18.19mm	0.2mm
S9A	18.19mm	0.2mm	S9B	17.49mm	0.2mm
M10A	17.49mm	0.2mm	M10B	16.80mm	0.2mm
S10A	16.80mm	0.2mm	S10B	16.11mm	0.2mm
M11A	16.11mm	0.2mm	M11B	15.42mm	0.2mm
S11A	15.42mm	0.2mm	S11B	14.72mm	0.2mm
M12A	14.72mm	0.2mm	M12B	14.03mm	0.2mm
S12A	14.03mm	0.2mm	S12B	13.34mm	0.2mm
M13A	13.34mm	0.2mm	M13B	12.64mm	0.2mm
S13A	12.64mm	0.2mm	S13B	11.95mm	0.2mm
M14A	11.95mm	0.2mm	M14B	11.26mm	0.2mm
S14A	11.26mm	0.2mm	S14B	10.57mm	0.2mm
M15A	10.57mm	0.2mm	M15B	9.87mm	0.2mm
S15A	9.87mm	0.2mm	S15B	9.18mm	0.2mm
M16A	9.18mm	0.2mm	M16B	8.49mm	0.2mm

Table 3.1 Patch A and Patch B measurements

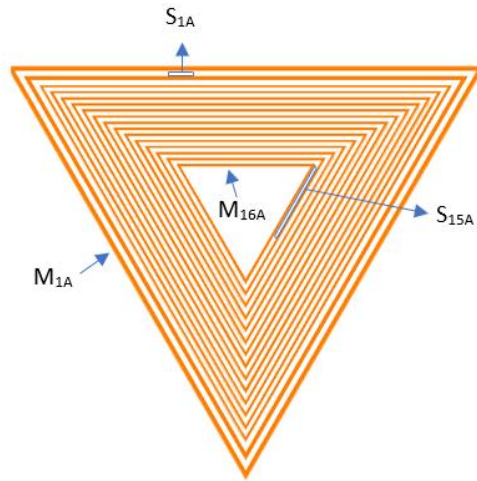


Fig 3.2. Patch A

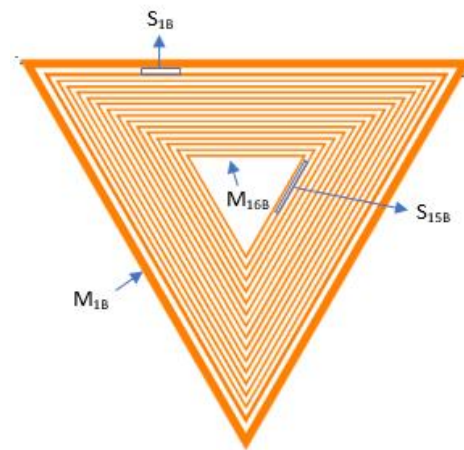


Fig 3.3. Patch B

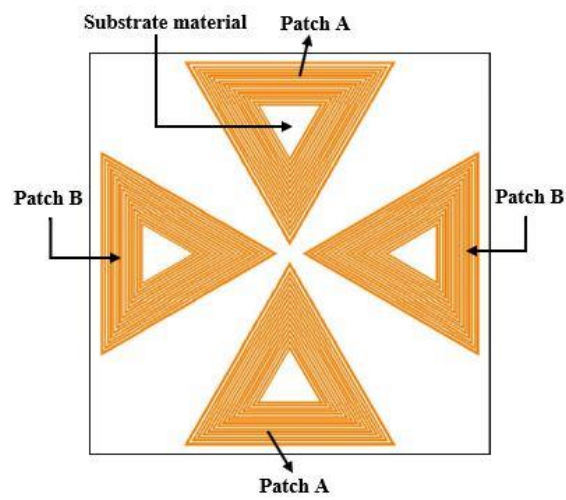


Fig 3.4. Presented Tag Design

## RESULTS AND DISCUSSIONS

The 30-bit claimed tag is optimised for various materials so that it can be utilized in the real world under various circumstances of environment. It can create  $2^{30} = 1073741824$  bits and has a high read range ability. Table 2 contrasts tags based on their various laminates, flexibility, radiators, operating bandwidth, and capabilities of sensing which is also an important feature. We will discuss each tag in detail in this chapter. Figure 4.1 and Figure 4.2 shows the simulated response of Patch A and Patch B respectively.

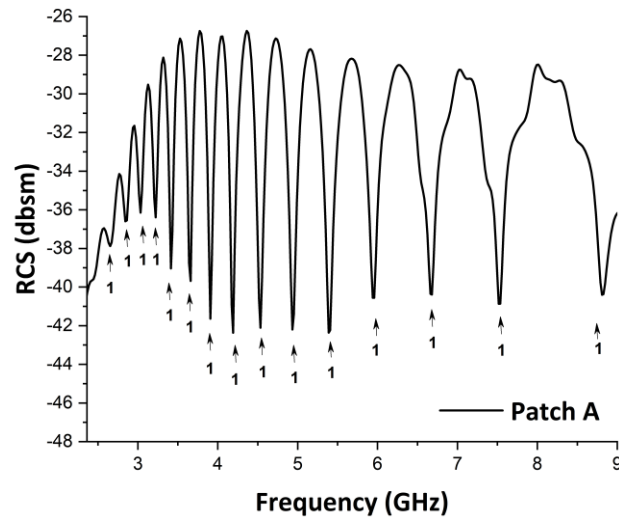


Fig 4.1. Simulated Result of Patch A

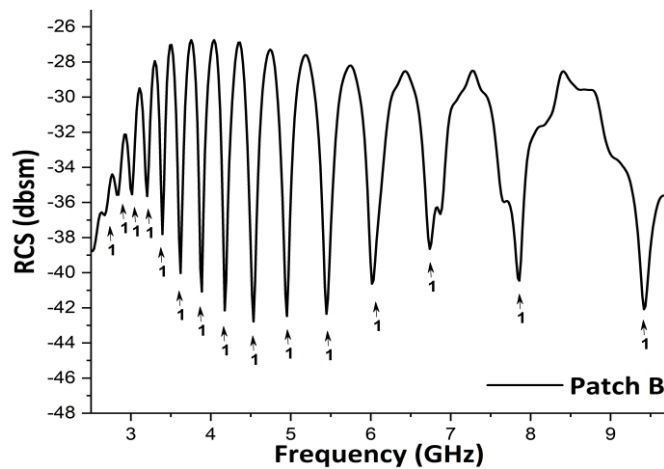


Fig 4.2. Simulated Result of Patch B

## 4.1 TAG-A

Copper serves as the radiator while Taconic TLX-8 serves as the substrate in Tag A. The tag exhibits the 30-bit means it is capable of tagging up to  $2^{30}$  objects. It uses the frequency band from 2.8 to 9.3 GHz, so it uses the bandwidth of almost 7.5 GHz. The substrate used in this tag is rigid and it can't be applied on flexible objects. It uses the same two patches named as patch A and patch B to generate 30 bits with the contribution of 15 bits from every patch. Figure 4.3 shows the simulated response of Tag A having the tag ID "111111111111111111111111111111". Utilizing CST microwave studio, simulated response of the tag is analyzed.

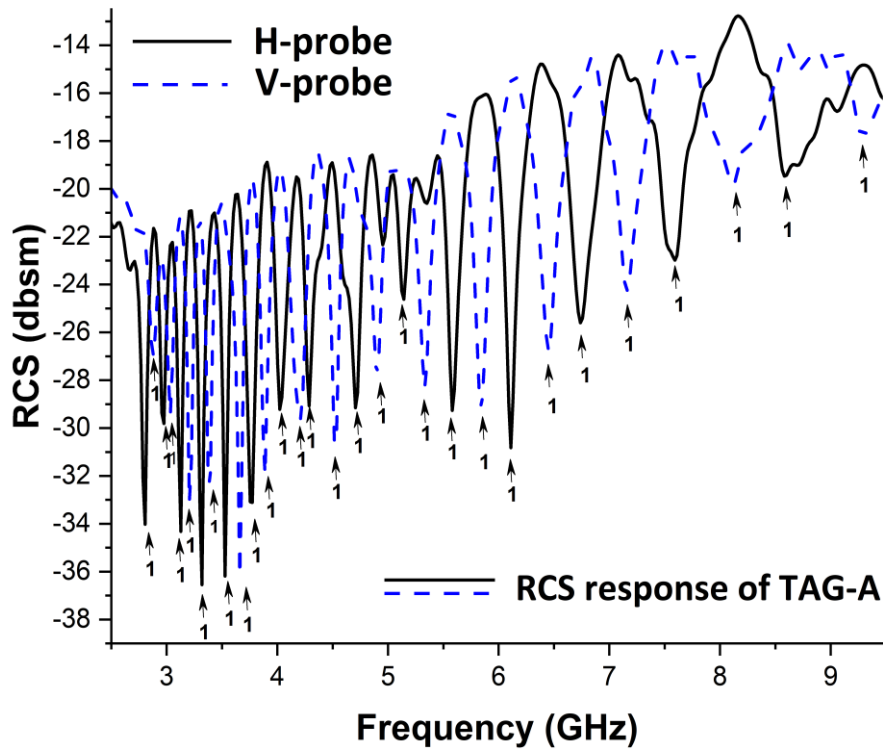


Fig 4.3. Simulated Result of TAG-A

## 4.2 TAG-B

Copper serves as the radiator and Rogers RT/Duroid® (5880) serves as the substrate for tag B. Rogers RT/Duroid/5880 is a bendable substrate and it has low moisture absorption. The substrate has the thickness of 0.508 mm while the copper has 0.035 mm thickness. The tag possesses the frequency response between 2.66 to 8.97 GHz means the tag response uses the bandwidth of 6.13 GHz. It also has the same data

encoding capacity of 30 bits. Figure 4.4 shows the simulated response of TAG-B.

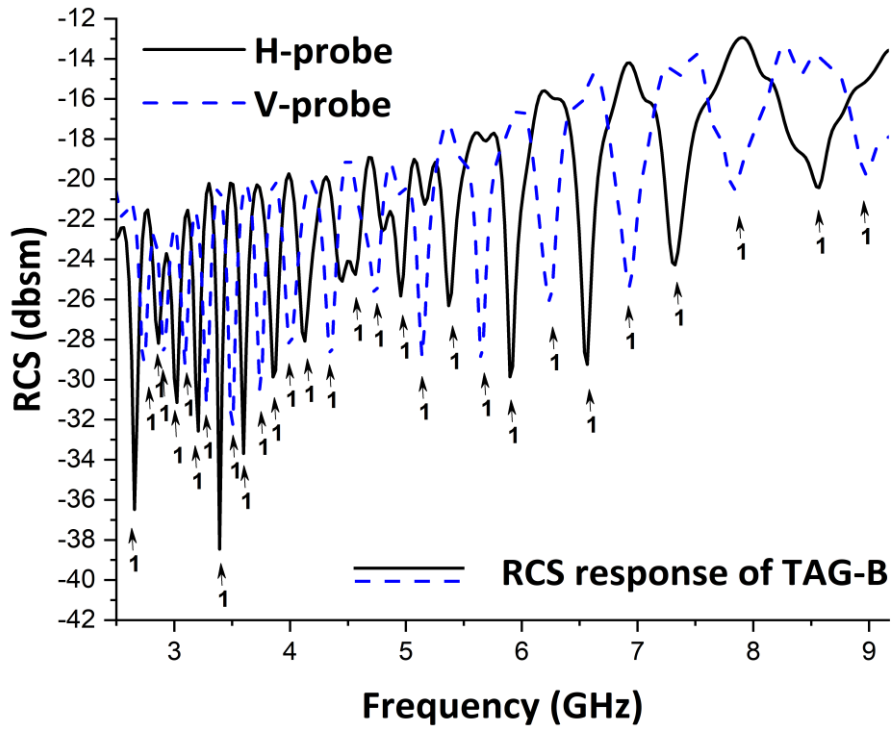


Fig 4.4. Simulated Result of TAG-B

### 4.3 TAG-C

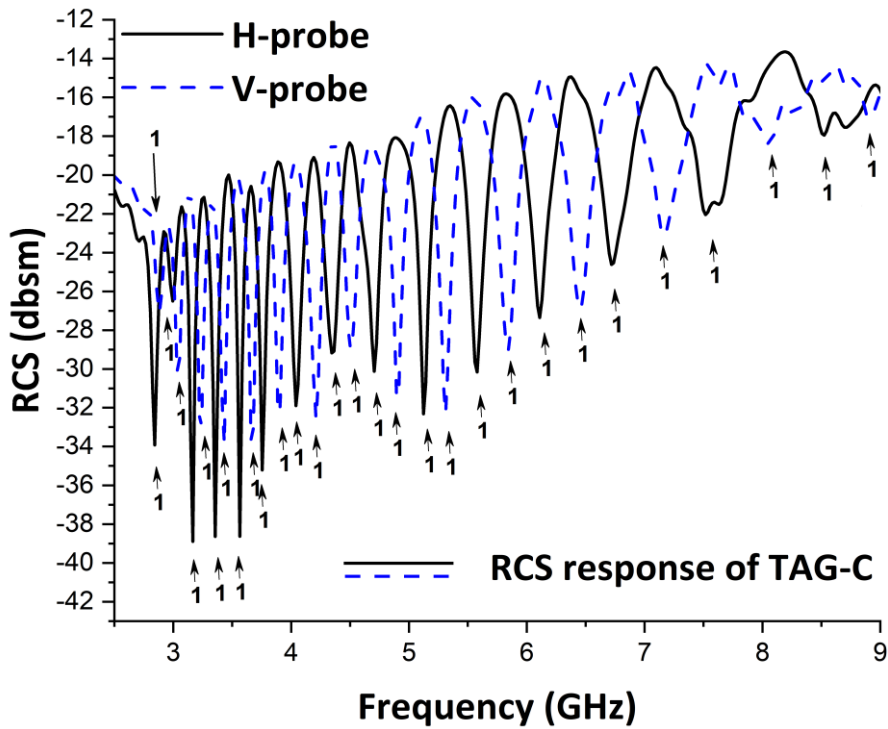


Fig 4.5. Simulated Result of TAG-C





## 4.5 TAG-E

Another flexible laminate called Kapton HN serves as the substrate for Tag, with silver nano ink serving as the radiator. Kapton HN is a thin polyimide film can be employed successfully in application over the wide range of temperature. It can operate between the  $-269^{\circ}\text{C}$  to  $400^{\circ}\text{C}$ . It also exhibits the sensitivity against humidity, which we will see later in this thesis. The substrate has a thickness of 0.127 mm and radiator has a thickness of 0.015 mm. This tag required the frequency range of 2.63 GHz to 9.22 GHz for its operation, so it uses the bandwidth of 6.5 GHz. The tag has the loss tangent of 0.0026 and relative permittivity of 3.5. Figure 14 shows the simulated response of TAG-E having the tag-ID of all “11111111111111111111111111111111”. Solid lines shows RCS response of tag w.r.t H-probe and dotted lines shows the response of tag w.r.t V-probe making overall the total 30-dips with the participation of 15-bits from each probe. The presence of dip in RCS response of tag indicates the 1's and absence of dip indicate the 0's. It is observed that the tag resonating dips varies between -15 to -33 dbsm along vertical axis. This tag can be employed on irregular surfaces as the substrate has the flexible nature. The tag also has the printability feature as the radiator used is Silver Nano Ink which can be printed using the laser jet printer.

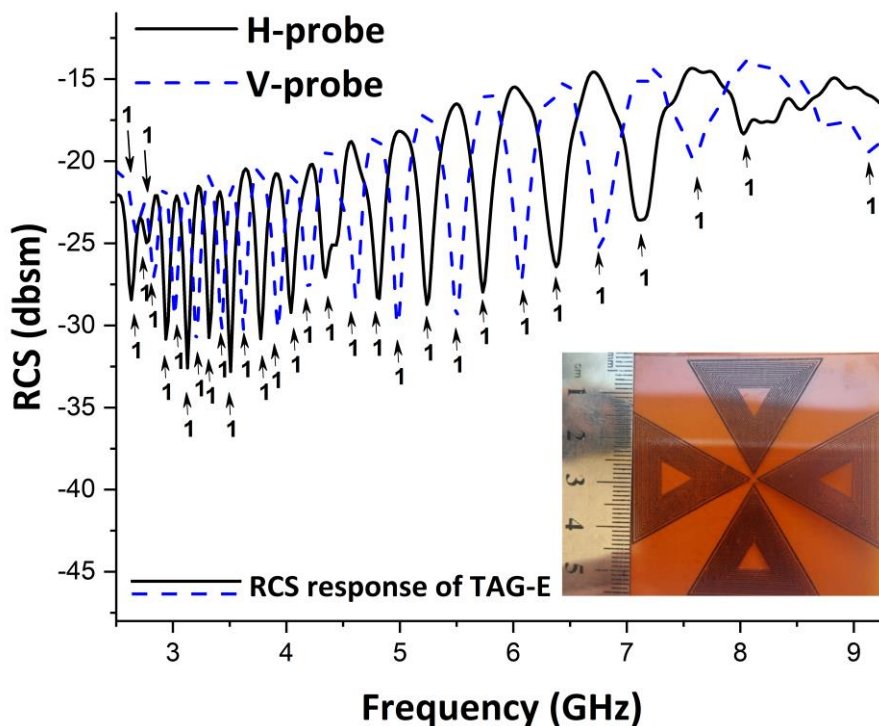


Fig 4.7 Simulated Result of TAG-E

The Cabot CCI-300 silver nano-ink-filled DMP2800 inkjet printer, as utilized in [54], is used to print the prototype Kapton® HN-based flexible tag. At 150°C, the printing process lasts for two hours. Additionally, the tag is examined with a Carl Zeiss NTS Ultra-55 Field Emission Scanning Electron Microscope for printing accuracy. Furthermore, inkjet printing is chosen for mass production due to its ability to adapt and for high throughput [55]. TAG-E prototype printed with inkjet printer is shown in Figure 4.7. Table 4.1 shows the TAG-E resonating frequencies by using formula mentioned in equation (2).

Patch A			Patch B		
Slots	Length	Frequency	Slots	Length	Frequency
S1A	30.31mm	2.63 GHz	S1B	29.27mm	2.7 GHz
S2A	28.23mm	2.79 GHz	S2B	27.19mm	2.85 GHz
S3A	26.50mm	2.94 GHz	S3B	25.81mm	3.01 GHz
S4A	25.11mm	3.13 GHz	S4B	24.42mm	3.20 GHz
S5A	23.73mm	3.34 GHz	S5B	23.04mm	3.45 GHz
S6A	22.34mm	3.55 GHz	S6B	21.65mm	3.66 GHz
S7A	20.96mm	3.80 GHz	S7B	20.26mm	3.96 GHz
S8A	19.57mm	4.1 GHz	S8B	18.88mm	4.23 GHz
S9A	18.19mm	4.42 GHz	S9B	17.49mm	4.64 GHz
S10A	16.80mm	4.84 GHz	S10B	16.11mm	5.03 GHz
S11A	15.42mm	5.26 GHz	S11B	14.72mm	5.54 GHz
S12A	14.03mm	5.77 GHz	S12B	13.34mm	6.09 GHz
S13A	12.64mm	6.4 GHz	S13B	11.95mm	6.79 GHz
S14A	11.26mm	7.18 GHz	S14B	10.57mm	7.68 GHz
S15A	9.87mm	8.1 GHz	S15B	9.18mm	9.22 GHz

Table 4.1 Resonating frequencies of TAG-E

Table 4.2 summarized the comparison of all tags in terms of flexibility, thickness, sensitivity, and printability etc. As mentioned earlier, the tag can be used for tagging  $2^{30}$  objects. For this we have optimized the tag for two more different tag IDs. Different tag IDs can be achieved by shorting the respective slots/resonators. Figure 4.8 shows the simulated response of tag ID “11101111111111111111111111111111” & Figure 4.9 shows the simulated response of tag ID “10101010101010101010101010101010”. In Figure 4.8, the shorted slot exhibits the bit “0” on that slot. Similarly, if we see in figure 4.9, all the V-probe slots show the all zero’s means we have shorted the all patch B slots to get the desired tag ID.

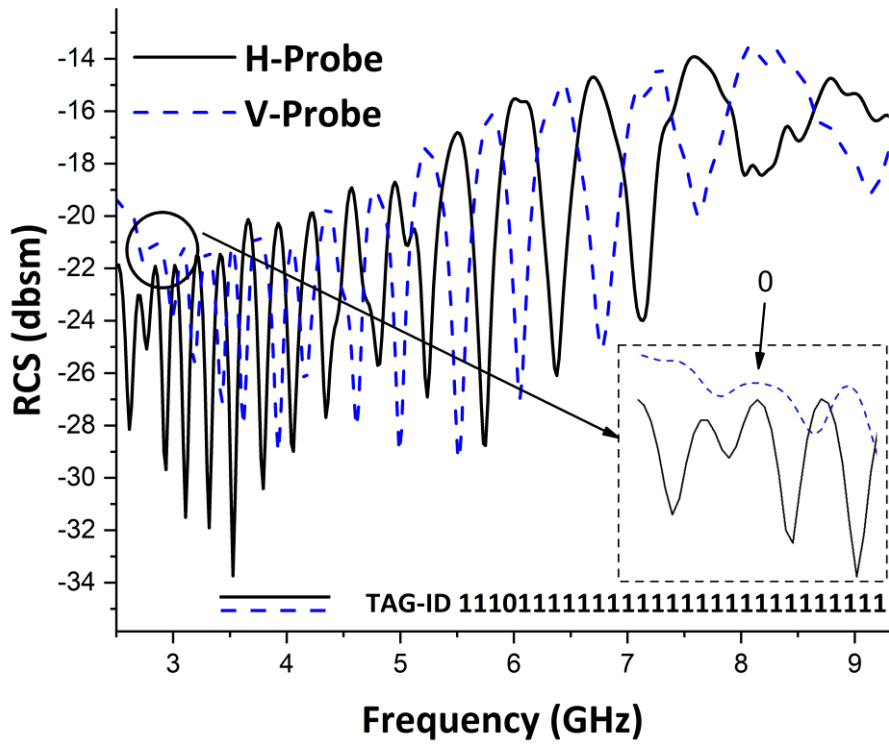


Fig 4.8. Simulated response of TAG-E with unique tag ID

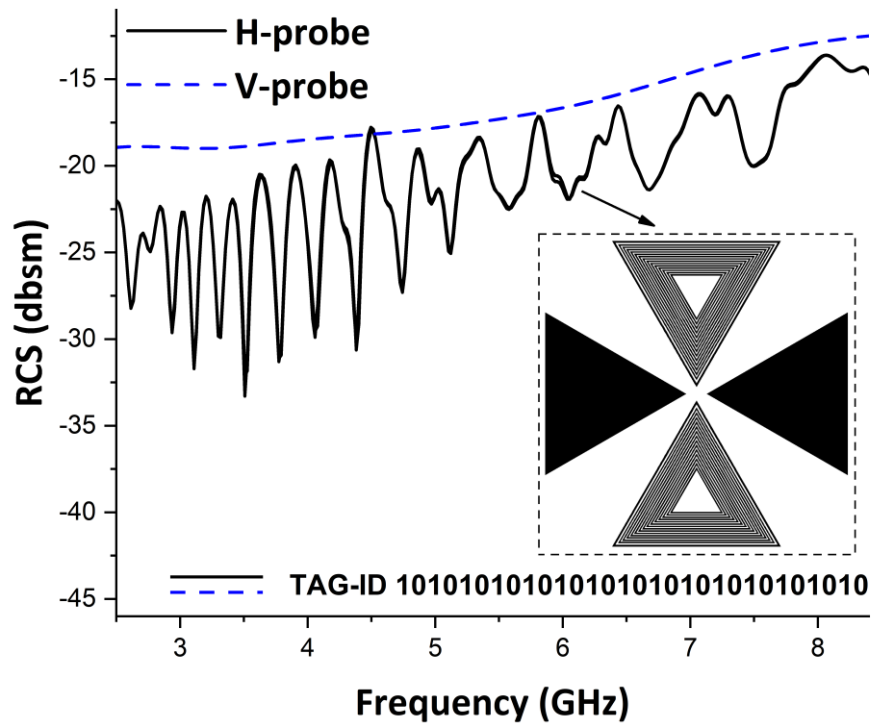


Fig 4.9. TAG-E simulated response with alternate 1's Tag ID

Parameters	TAG-A	TAG-B	TAG-C	TAG-D	TAG-E
<b>Substrate</b>	Taconic (TLX-8)	Rogers RT/Duroid® (5880)	Taconic (TF290)	PET	Kapton® HN
<b>Radiator</b>	Copper	Copper	Copper	Silver Nano ink	Silver Nano ink
<b>Sub.Thickness (mm)</b>	0.13mm	0.508mm	0.09mm	0.1mm	0.127mm
<b>Rad.Thickness</b>	0.035mm	0.035mm	0.035mm	0.015mm	0.015mm
<b>Relative permittivity</b>	2.55	2.2	2.9	2.9	3.5
<b>Loss Tangent</b>	0.0017	0.0009	0.0028	0.0025	0.0026
<b>Bandwidth</b>	6.93 GHz	6.31 GHz	6.07 GHz	6.41GHz	6.59 GHz
<b>Total bits</b>	30	30	30	30	30
<b>Size</b>	55.3mm x 55.3mm	55.3mm x 55.3mm	55.3mm x 55.3mm	55.3mm x 55.3mm	55.3mm x 55.3mm
<b>Flexibility</b>	No	Yes	Yes	Yes	Yes
<b>Sensing</b>	No	No	No	No	Yes
<b>Printability</b>	No	No	No	Yes	Yes

Table 4.2. Tag's comparison with different laminates/substrates

#### 4.5.1 Humidity Sensing

The humidity sensing capability of TAG-E is also available, and it works by utilizing a Kapton HN property. After being exposed to a moist atmosphere that changes, Kapton HN exhibits a change in relative permittivity. According to Ref [56], the equation (4) determines how the change in relative humidity affect the Dupont Kapton® HN polyamide thin film properties in term of relative permittivity.

$$Er = 3.05 + 0.008 \times RH \quad (4)$$

According to equation (4), the relative permittivity of the polyamide thin film evolves when the relative humidity changes from 0% to 100%, it goes from 3.05 to 3.85. Using equation (4), the relative permittivity for 60% is calculated as follows.

$$Er = 3.05 + 0.008 \times 60$$

$$Er = 3.53$$

According to equation (4), the relative permittivity of the tag shoot up as relative

humidity does. As a result, the correspondence described in equation (2) causes a modest shift in the simulated response of the tag towards the lower frequencies.

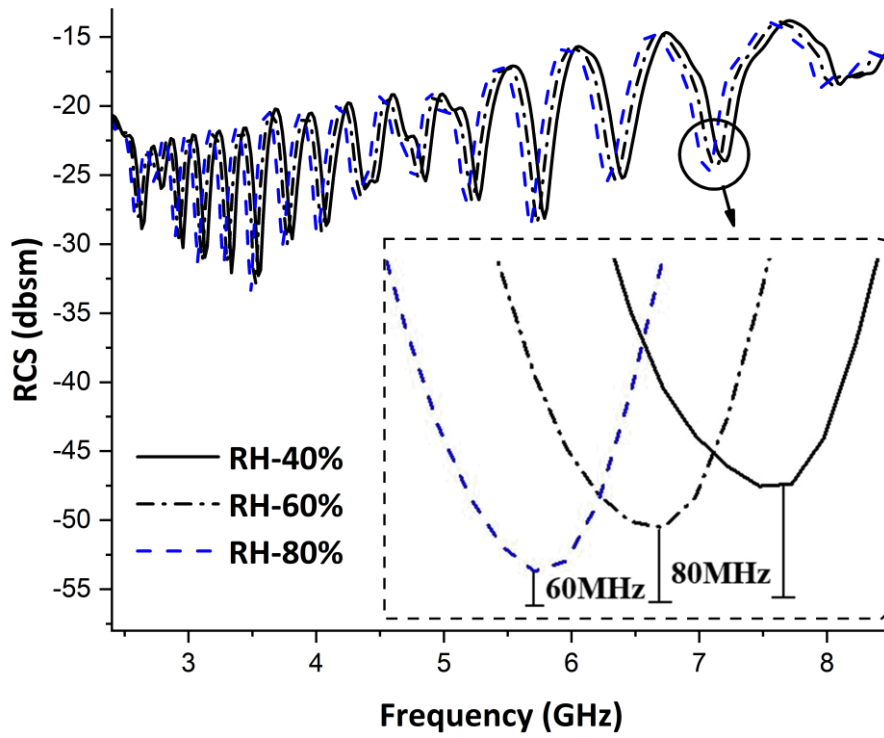


Fig 4.10. Computed RH response using H-probe only

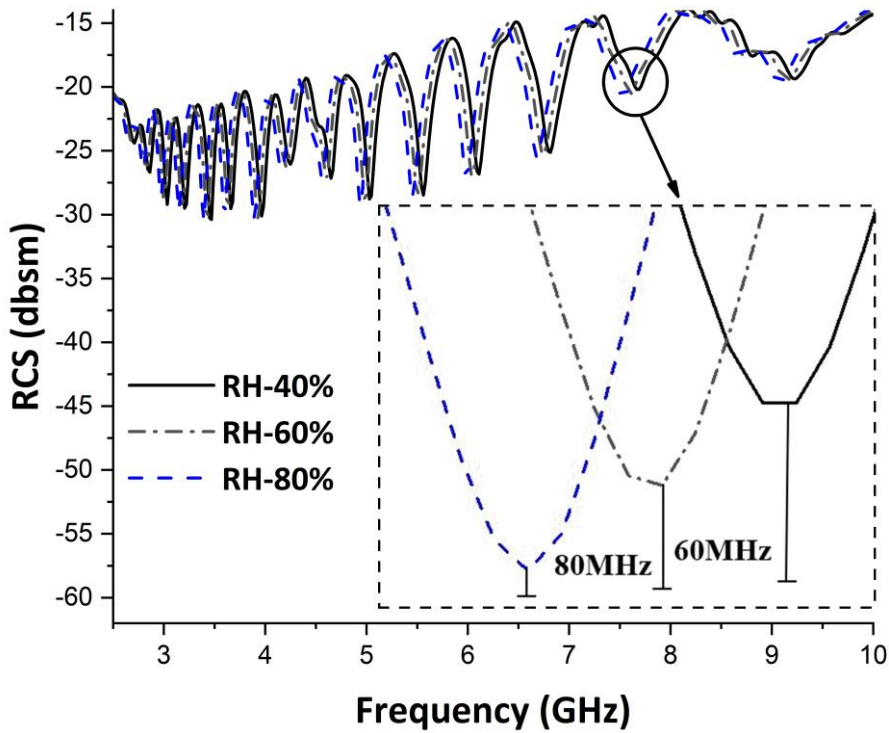


Fig 4.11 Computed RH response using V-probe only

The computed response of relative humidity (RH) with respect to the H-probe is shown in Figure 4.10. It is clear from the figure that as the RH changed from 40% to 60%, the relative permittivity changed from 3.37 to 3.69, which caused the RCS response to vary. When the relative permittivity changes from 3.37 to 3.69, an average shift of 70 MHz is seen towards lower frequencies. The estimated response of relative humidity (RH) with respect to the V-probe is shown in Figure 4.11, where a 70 MHz change in frequency is seen towards the lower frequencies.

#### 4.5.2 Experimental Setup for Humidity Sensing

Utilizing the environmental room of dimensions 50 x 34 x 36 cm<sup>3</sup> as used in Ref [33], it is possible to measure the sensory response to humidity. The airtight plastic box contains the suggested s a water spray bottle, sensor tag, , two horn antennas, and a commercial sensor. The VNA (Agilent Tech E5071C) is positioned at a height of 25 cm to collect the measured results, and the tag is kept 39 mm (far-field distance) away from the horn antennas. To improve the tag's overall RCS response, equation (5) is applied.

$$\sigma^{tag} = \left[ \frac{s_{11}^{tag} - s_{11}^{isolation}}{s_{11}^{ref} - s_{11}^{isolation}} \right] \sigma^{ref} \quad (5)$$

Where  $s_{11}^{tag}$  is the claimed sensor tag's reflection coefficient and  $s_{11}^{ref}$  and  $s_{11}^{isolation}$ , are the reference reflection coefficient of metallic plate and an antenna's reflection coefficient without tag and the reference metallic plate respectively. While  $\sigma^{ref}$  the proposed tag's RCS response. The humidity measured response of the H-probe and V-probe are shown in Figures 4.12 and 4.13, respectively. As soon as the water is sprayed within the chamber, it becomes apparent that the relative humidity level comes up, changing the electrical characteristics of the Kapton® HN- substrate based tag and producing a little shift towards lower frequencies. Because of external influences and the narrow spacing of the slots, ripples can be noticeable in measured response. The fringing effect has also been found to create an insignificant shift in frequency response, which can be overcome by signal processing techniques as mentioned earlier.

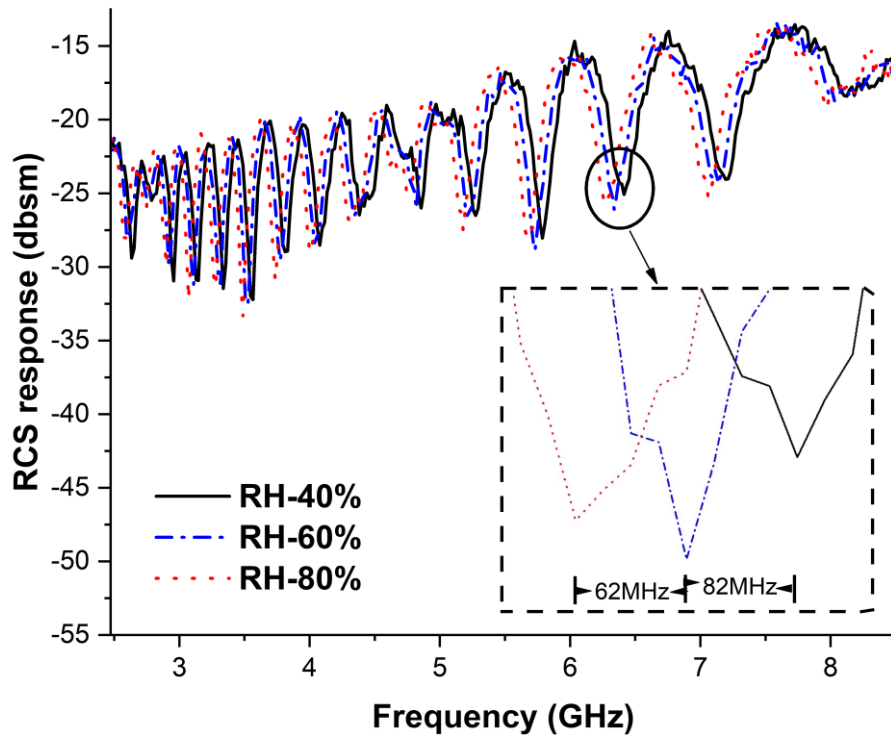


Fig 4.12. Measured humidity sensing graph w.r.t H-probe

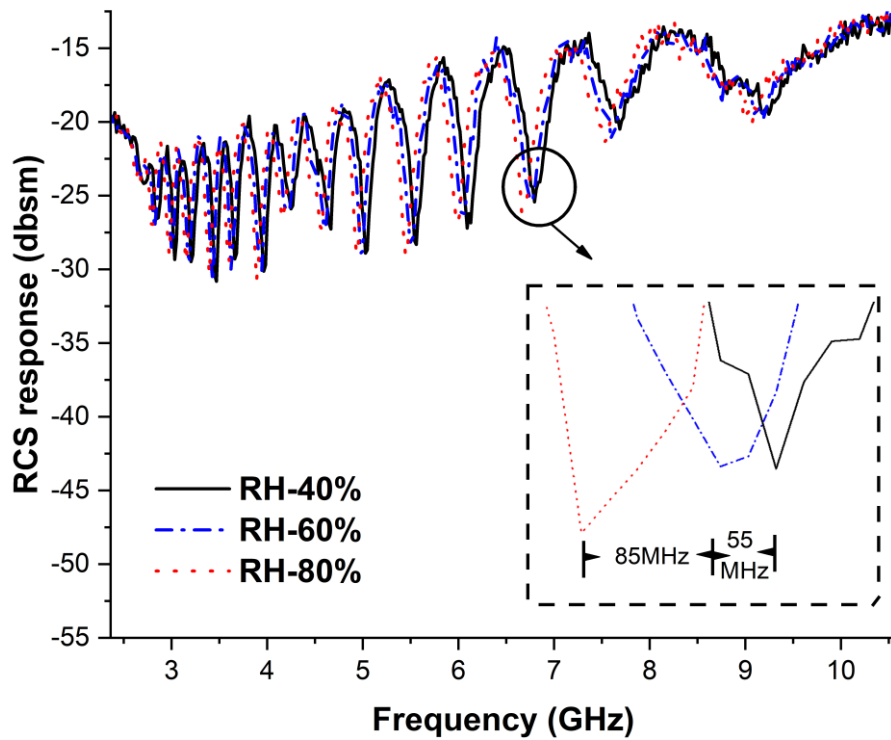


Fig 4.13. Measured humidity sensing graph w.r.t V-probe

## 4.6 Comparison with previous state of art tags

The suggested tag has been collating with the prior generation, chipless RFID tags in Table 4.3. This table examines various essential aspects of the proposed work and similar research to explain its originality. The suggested tag's primary characteristics are its characteristic properties, which include higher data density, effective band utilization, adaptability, sensing and high spectral capacity. The material used to create the realized sensor tag is sturdy and trustworthy, allowing it to be used in demanding environments. If we see from the below Table 4 the tag presented in reference [40] has the encoding capacity of 6 bits and has the sensing and flexibility feature because the substrate used is flexible, but the spectral density is very low and mass production is also difficult. If we see the reference [57], this tag has better bit density from the tag presented in [40], but the tag has no flexibility feature and very low encoding capacity, similar case for others referred tags. The proposed tag has efficient bandwidth utilization, better encoding and spectral capacity from the tags proposed in literature review.

Ref []	Bits	Bandwidth	Flex- ibility	Sens- ing	Spectral Capacity (Bits/GHz)	Bit density (bits/cm <sup>2</sup> )	Mass Productio n
[34]	6	6.5 GHz	Yes	Yes	0.92	0.24	Difficult
[57]	7	6 GHz	No	Yes	0.86	1.33	Suitable
[36]	18	6.5 GHz	No	No	2.77	0.7	Difficult
[58]	8	3 GHz	No	No	2.67	4	Difficult
[59]	3	4.5 GHz	No	Yes	0.67	0.48	Difficult
Propos ed work	30	6.59 GHz	Yes	Yes	4.55	0.99	Suitable

Table 4.3 Comparison with already presented tags



### **CONCLUSION**

The primary objective of this research is to design an economical, eco-friendly, versatile, and reliable Chipless RFID tag with integrated sensors. All the targeted goals and objectives are achieved, and the summaries of the research outcomes are highlighted in this section.

Chapter 1 refers to a brief introduction of IoT and present and the future scope of IoT. It also highlighted the scope of the Chipless RFID tags with integrated sensor concerning some recent reports. Considering the present horizon of Chipless RFID sensors with respect to current statistics, these state-of-the-art nodes are the core domain of this research work. A short background is also shared to show the prominence of tag in IoT market.

In the second chapter different types of Chipless RFID tags which was previously presented in recent years discussed to clearly understand the research behind choosing the Chipless RFID tag. Different recently published papers are discussed one by one to elaborate the scope of our research. In Chapter 2, the requirement for creating far more advanced prototypes with the most benefits is demonstrated by comparing the suggested study to the previously published work.

The third chapter compiled different types of chipless RFID tags. The working theory and tag designing methods are explained with references to several chipless tags that have previously been created. The chapter aids the reader in comprehending the fundamental design of chipless RFID sensors in relation to pertinent work. In Chapter 3, the requirement for creating far more advanced prototypes with the most benefits is demonstrated by comparing the suggested study to the previously published work. In 3<sup>rd</sup> chapter also, proposed research work is also explained in detail with proposed tag design.

Chapter 4 explains the simulation result of every tag in detail which was optimized on different substrates. The reader will be able to determine which types of sensing materials are best for their intended use with the aid of this examination. A complete and in-depth analysis of all relevant sensing data presented in tabular form might help

the researcher select the best course of action. The materials used in designing different types of substrates have different properties which show changes into the different factors. So, the tags can be used in different environmental conditions based in the real-world requirement or we can say based on the requirements of applications. Moreover, bendable, and flexible laminates are also employed so that the tag proposed can be used on irregular surface. The optimized tag has such features which is not presented earlier in the literature review tags. In the chapter, also the sensitivity of the tag is also achieved by utilizing the property of laminate which shows the change in its properties when it faces different environmental conditions. In the last the novelty of the tag is explained by comparing the tag with the previously presented tags in tabular form. We can summarize overall conclusion as below.

A 30-bit dual-polarized star-shaped tag is presented in the study work. The tag structure is created and tailored for various substrate materials and radiator types. Silver nanoparticles are used as the resonating material combined with Dupont Kapton® HN polyamide film to create a fully printed sensor. It was found that a frequency shift took place as RH rise from 40% to 80%. It is concluded that this tag achieves sensing capability without integrating an external sensor, along with better spectral capacity than previously presented state of the art tags. The encoded bits are obtained using the frequency coding approach. Patches are replicated in a fan-like pattern to increase the tag's reading sensitivity. Compared to the tags described in the literature review, the presented tag has a wider reading range and more data bits with efficient band utilization. The printed sensor tag is the best option for use in low-cost tagging applications that also require sensing.

## **5.1 Future Work**

An rise in RF wave concentration in a network is caused by the interconnectedness of every component in the ubiquitous network. Each node's RF waves for data transfer have the potential to clash with one another. Data loss may occur as a result of this collision. Better anti-collision algorithms will be able to stop data collision in the future, preventing any data loss [60]. The straightforward circuitry of passive RFID tags cannot support extra processing units. The RF communication in this instance is therefore susceptible to spoofing and eavesdropping. To complement affordable, dependable RFID devices, improved, more lightweight cryptographic methods are

therefore required. In case of our case which are passive tags these simple structure are not enough for processing units and may vulnerable to spoofing, so low cost cryptographic protocols need to be implemented to make these low cost RFID systems more reliable in future.

Also in future the use of environmental friendly substrates for chipless RFID tag is also highly appreciated to avoid the toxic emission during tag fabrication. It is expected that Machine Learning (ML) algorithms will also be used to read the EM signatures. With the help of ML algorithm, it will be easy to make the RFID system more intelligent.

## BIBLIOGRAPHY

- [1] Swamy, S. Narasimha, S.R Kota “An Empirical Study on System Level Aspects of Internet of Things (IoT),” *IEEE Access*, vol. 8. pp. 188082-188134, 2020.
- [2] A. Habib, et al. "Data dense chipless RFID tag with efficient band utilization." *AEU-International Journal of Electronics and Communications*, p.154220, 2022.
- [3] S. Zeb, A. Habib, Y. Amin, et al “Green Electronic Based Chipless Humidity Sensor for IoT Applications,” *IEEE Green Technologies Conference (Greentech)*, pp. 172-175, 2018.
- [4] N. Javed et al., “The Effect of IoT New Features on Security and Privacy: New Threats, Existing Solutions, and Challenges Yet to Be Solved,” *IEEE Internet of Things Journal*, vol. 6, no. 2, pp. 1606-1616, 2019.
- [5] The statistics portal Internet of Things (IoT) Connected Devices Installed Base Worldwide From 2015 to 2025 (in Billions), 2017. [Online]. Available at: <https://www.statista.com/statistics/471264/iotnumber-of-connected-devices-worldwide/>
- [6] <https://www.idtechex.com/en/research-report/sensors-2021-2041/761>
- [7] <https://www.idtechex.com/en/research-report/wearable-sensors-2021-2031/780>
- [8] <https://www.idtechex.com/en/research-report/printed-and-flexible-sensors-2020-2030-technologies-players-forecasts/755>
- [9] <https://www.idtechex.com/en/research-report/smart-and-intelligent-packaging-2020-2030/691>
- [10] Ling-yuan Zeng, ”A Security Framework for Internet of Things Based on 4G Communication,” in *Computer Science and Network Technology (ICCSNT)*, 2012, pp. 1715-1718.
- [11] Guicheng Shen and Bingwu Liu, ”The visions, technologies, applications and security issues of Internet of Things,” in *E-Business and E -Government (ICEE)*, 2011, pp. 1-4.
- [12] Xu Cheng, Minghui Zhang, Fuquan Sun,” Architecture of internet of

- things and its key technology integration based-on RFID,” in Fifth International Symposium on Computational Intelligence and Design, pp. 294-297, 2012.
- [13] Farooq, M. Umar, et al. "A review on internet of things (IoT)." *International journal of computer applications* 113.1 (2015): 1-7.
- [14] Debasis Bandyopadhyay, Jaydip Sen, "Internet of Things - Applications and Challenges in Technology and Standardization" in *Wireless Personal Communications*, Volume 58, Issue 1, pp. 49-69.
- [15] Ying Zhang, "Technology Framework of the Internet of Things and Its Application," in *Electrical and Control Engineering (ICECE)*, 2011, pp. 4109-4112.
- [16] MiaoWu, Ting-lie Lu, Fei-Yang Ling, ling Sun, Hui-Ying Du, "Research on the architecture of Internet of things," in *Advanced Computer Theory and Engineering (ICACTE)*, 2010, pp. 484-487.
- [17] Rafiullah Khan, Sarmad Ullah Khan, Rifaqat Zaheer and Shahid Khan, "Future Internet: The Internet of Things Architecture, Possible Applications and Key Challenges," in *Proceedings of Frontiers of Information Technology (FIT)*, 2012, pp. 257-260.
- [18] A. A. Awan, M. N. Salimi, M. A. Riaz, H. Shahid, M. A. Asghar, and Y. Amin, "An rfid enabled miniaturized chipless tag for iot applications," in *2020 IEEE 23rd International Multitopic Conference (INMIC)*, 2020, pp. 1-5.
- [19] <https://www.marketsandmarkets.com/Market-Reports/rfid-market-446.html>
- [20] S. J. Thomas, "Rfid for everyone: An easily-accessible, experimental uhf rfid platform," *IEEE Journal of Radio Frequency Identification*, vol. 4, no. 1, pp. 46-54, 2020
- [21] S. Ziegler, S. Nikoletsea, S. Krco, J. Rolim and J. Fernandes, "Internet of Things and crowd sourcing - a paradigm change for the research on the Internet of Things," *2015 IEEE 2nd World Forum on Internet of Things (WF-IoT)*, Milan, 2015, pp. 395-399.

- [22] J. Voas, B. Agresti and P. A. Laplante, "A Closer Look at IoT 's Things," in *IT Professional*, vol. 20, no. 3, pp. 11-14, May./Jun. 2018.
- [23] S. K. Vishwakarma, P. Upadhyaya, B. Kumari and A. K. Mishra, "Smart Energy Efficient Home Automation System Using IoT," *2019 4th International Conference on Internet of Things: Smart Innovation and Usages (IoT-SIU)*, Ghaziabad, India, 2019, pp. 1-4, doi: 10.1109/IoT-SIU.2019.8777607.
- [24] I. Balbin and N. C. Karmakar, "Phase-encoded chipless RFID transponder for large-scale low-cost applications", *IEEE Microwave and Wireless Components Letters*, vol. 19, no. 8, pp. 509–511, 2009.
- [25] B. Shao, Q. Chen et al., "Design of Fully printable and Configurable Chipless RFID Tag on Flexible Substrate," *Microwave and Optical Technology Letters*, vol. 54, no. 1, pp. 226-230, January 2010.
- [26] B. Shao et al., "An ultra-low-cost RFID Tag with 1.67Gbps Data Rate by Inkjet Printing on Paper Substrate," in *IEEE Asian Solid-State Circuit Conference (A-SSCC)*, 2010.
- [27] X. Qing, C. K. Goh, and Z. N. Chen, "Impedance characterization of RFID tag antennas and application in tag co-design", *IEEE Trans. on Microw. Theory and Techniques*, vol. 57, no. 5, pp. 1268–1274, 2009.
- [28] D. M. Dobkin, "The RF in RFID: Passive UHF RFID in Practice", Elsevier Science, 2007.
- [29] A. Ren, A. Zahid, M. A. Imran, A. Alomainy, D. Fan and Q. H. Abbasi, "Terahertz Sensing for Fruit Spoilage Monitoring," *2019 Second International Workshop on Mobile Terahertz Systems (IWMTS)*, Bad Neuenahr, Germany, 2019, pp. 1-4, doi: 10.1109/IWMTS.2019.8823735
- [30] A. Ren, A. Zahid, M. A. Imran, Q. H. Abbasi and A. Alomainy, "Monitoring Quality Control of Fruits Using Terahertz Sensing," *2019 IEEE International Symposium on Antennas and Propagation and USNC-URSI Radio Science Meeting*, Atlanta, GA, USA, 2019, pp. 381-382, doi: 10.1109/APUSNCURSINRSM.2019.8888479.
- [31] R. K. Kanth *et al.*, "Information and communication system technology's impacts on personalized and pervasive healthcare: A

- technological survey," *2014 IEEE Conference on Norbert Wiener in the 21st Century (21CW)*, Boston, MA, USA, 2014, pp. 1-5, doi: 10.1109/NORBERT.2014.6893917.
- [32] G. Yang, et al, "Bio-Patch Design and Implementation Based on a Low-Power System-on-Chip and Paper-Based Inkjet Printing Technology," in *IEEE Transactions on Information Technology in Biomedicine*, vol. 16, no. 6, pp. 1043-1050, Nov. 2012, doi: 10.1109/TITB.2012.2204437.
- [33] N. Javed, M. A. Azam, I. Qazi, Y. Amin and H. Tenhunen, "Data-Dense Chipless RFID Multisensor for Aviculture Industry," in *IEEE Microwave and Wireless Components Letters*, vol. 30, no. 12, pp. 1193-1196, Dec. 2020, doi: 10.1109/LMWC.2020.3032027.
- [34] L. Shahid, H. Shahid, M.A. Riaz, et al., "Chipless RFID Tag for Touch Event Sensing and Localization", *IEEE Access*, vol. 8, pp. 502-513, 2020.
- [35] H. Shahid, M.A. Riaz, Y. Amin, et al. Novel QR-incorporated chipless RFID tag. *IEICE Electronics Express*, pp.16-20180843, 2019.
- [36] G. Khadka, M. A. Bibile, L. M. Arjomandi, et.al, "Analysis of Artifacts on Chipless RFID Backscatter Tag Signals for Real World Implementation", *IEEE Access*, vol. 7, pp. 66821-66831, 2019.
- [37] P. Prabavathi and S. Subha Rani, "Flower shaped frequency coded chipless rfid tag for low cost item tracking." *Analog Integrated Circuits and Signal Processing*, vol. 109, pp. 79–91, 2021.
- [38] W. M. Adbulkawi and A.-F. A. Sheta, "Printable chipless rfid tags for iot applications," in *2018 1st International Conference on Computer Applications Information Security (ICCAIS)*, 2018, pp. 1–4.
- [39] M. Added, N. Boulejfen, M. Svanda, F. M. Ghannouchi, and T.-P. Vuong, "High-performance chipless radio-frequency identification tags: Using a slow-wave approach for miniaturized structure," *IEEE Antennas and Propagation Magazine*, vol. 61, no. 4, pp. 46–54, 2019.
- [40] M. S. Hashmi and V. Sharma, "Design, analysis, and realization of chipless RFID tag for orientation independent configurations" *Eng. J.*, vol. 2020, no. 5, pp. 189–196, Jan. 2020.

- [41] I. Jabeen, A. Ejaz, A. Akram, Y. Amin, J. Loo, H. Tenhunen, and Y. Amin, "Elliptical slot based polarization insensitive compact and flexible chipless rfid tag," *International Journal of RF and Microwave Computer-Aided Engineering*, 11 2019.
- [42] N. Javed, M. A. Azam, I. Qazi, Y. Amin, and H. Tenhunen, "A novel multi-parameter chipless rfid sensor for green networks," *AEU - International Journal of Electronics and Communications*, vol. 128, p. 153512, 2021.
- [43] Paredes, F.; Herrojo, C.; Mata-Contreras, J.; Moras, M.; Núñez, A.; Ramon, E.; Martín, F. Near-field chipless radio-frequency identification (RFID) sensing and identification system with switching reading. *Sensors* **2018**, 18, 1148.
- [44] Alam, J.; Khaliel, M.; Fawky, A.; El-Awamry, A.; Kaiser, T. Frequency-Coded Chipless RFID Tags: Notch Model, Detection, Angular Orientation, and Coverage Measurements. *Sensors* **2020**, 20, 1843.
- [45] Nguyen, D.H.; Zomorodi, M.; Karmakar, N.C. Spatial-Based Chipless RFID System. *IEEE J. Radio Freq. Identif.* 2019, 3, 46–55.
- [46] Babaeian, F.; Karmakar, N.C. Hybrid Chipless RFID Tags—A Pathway to EPC Global Standard. *IEEE Access* 2018, 6, 67415–67426.
- [47] J. Havlicek, M. Svanda, M. Polivka, et al. "Chipless RFID Tag Based on Electrically Small Spiral Capacitively Loaded Dipole", *IEEE Antennas and Wireless Propagation Letters*, vol. 16, pp. 3051-3054, 2017.
- [48] N. Javed, M.A. Azam, I. Qazi, Y. Amin, H. Tenhunen, "A novel multi-parameter chipless RFID sensor for green networks" *AEU-International Journal of Electronics and Communications*, 128, p.153512, 2021.
- [49] W.M. Abdulkawi, A.F.A. Sheta, K. Issa, et al. "Compact printable inverted-M shaped chipless RFID tag using dual-polarized excitation" *Electronics*, 8(5), p.580, 2019.
- [50] C. Herrojo, F. Paredes, J. Mata-contreras, et al. "Chipless-RFID: A review and recent developments", *Sensors*, 19(15), p.3385, 2019.



- [51] Mishra, R., P. Kuchhal, and A. Kumar. "Effect of Height of the Substrate and Width of the Patch on the Performance Characteristics of Microstrip Antenna." *International Journal of Electrical and Computer Engineering* 5.6,2015.
- [52] N. Javed, A. Habib, Y. Amin, et al. "Miniaturized flexible chipless RFID tag for IoT market", *International Conference on Communication, Computing and Digital Systems (C-CODE)*, pp. 71-74, 2017.
- [53] H. Anam, A. Habib, S.I. Jafri, et al. "Directly printable frequency signaturred chipless RFID tag for IoT applications". *Radioengineering*, 26(1), pp.139-146, 2017.
- [54] S. Zeb et al. "Polarization Insensitive Compact Chipless RFID Tag." *The Applied Computational Electromagnetics Society Journal (ACES)* pp. 312-318, 2018.
- [55] Y. Feng et al. "Low-cost printed chipless RFID humidity sensor tag for intelligent packaging." *IEEE Sensors Journal* 15.6: 3201-3208, 2014.
- [56] Mishra, R., P. Kuchhal, and A. Kumar. "Effect of Height of the Substrate and Width of the Patch on the Performance Characteristics of Microstrip Antenna." *International Journal of Electrical and Computer Engineering* 5.6,2015.
- [57] N. Javed, M. A. Azam, Y. Amin "Chipless RFID Multisensor for Temperature Sensing and Crack Monitoring in an IoT Environment", *IEEE Sensors Letters*, vol. 5, no. 6, pp. 1-4, 2021.
- [58] M. S. Hashmi and V. Sharma, "Design, analysis, and realization of chipless RFID tag for orientation independent configurations", *Eng. J.*, vol. 2020, no. 5, pp. 189–196, Jan. 2020.
- [59] T. Athauda and N. C. Karmakar, "The realization of chipless RFID resonator for multiple physical parameter sensing," *IEEE Internet Things J.*, vol. 6, no. 3, pp. 5387–5396, Jun. 2019.
- [60] R. K. Pateriya, S. Sharma, "The Evolution of RFID Security and Privacy: A Research Survey," *2011 International Conference on Communication Systems and Network Technologies (CSNT)*, pp.115-

119, June 2011.